

**UNCLASSIFIED**

---

---

**AD 284 914**

*Reproduced  
by the*

**ARMED SERVICES TECHNICAL INFORMATION AGENCY  
ARLINGTON HALL STATION  
ARLINGTON 12, VIRGINIA**



---

---

**UNCLASSIFIED**

NOTICE: When government or other drawings, specifications or other data are used for any purpose other than in connection with a definitely related government procurement operation, the U. S. Government thereby incurs no responsibility, nor any obligation whatsoever; and the fact that the Government may have formulated, furnished, or in any way supplied the said drawings, specifications, or other data is not to be regarded by implication or otherwise as in any manner licensing the holder or any other person or corporation, or conveying any rights or permission to manufacture, use or sell any patented invention that may in any way be related thereto.

63-1-1

NOLTR 62-35

APPROVED BY ASTIA  
Ref ID No.

284914

SUPersonic AERODYNAMIC HEAT TRANSFER  
AND PRESSURE DISTRIBUTIONS ON A SPHERE-  
CONE MODEL AT HIGH ANGLES OF YAW

- RELEASED TO ASTIA  
BY THE NAVAL ORDNANCE LABORATORY
- Without restrictions
  - For Release to Military and Government Agencies Only.
  - Approval by BuWeps required for release to contractors.
  - Approval by BuWeps required for all subsequent release.

8 JUNE 1962

NOL

UNITED STATES NAVAL ORDNANCE LABORATORY, WHITE OAK, MARYLAND

NOLTR 62-35

284914

JUN 1962

NOLTR 62-35

Aerodynamics Research Report No. 174

SUPersonic AERODYNAMIC HEAT TRANSFER AND  
PRESSURE DISTRIBUTIONS ON A SPHERE-CONE  
MODEL AT HIGH ANGLES OF YAW

by

Lionel Pasiuk

ABSTRACT: Measurements of the static pressure and aerodynamic heat transfer on the surface of a sphere-cone model at Mach numbers of 3.23 and 4.83, and angles of yaw of 6° and 18° have been made. The results of several theoretical methods for calculating both the laminar and turbulent heat transfer to the body along the most windward and leeward streamlines are compared with the experimental measurements. The experimental laminar heat-transfer distributions are nearly alike for the two Mach numbers, when they are expressed in the form of the Nusselt number divided by the square root of the Reynolds number. The experimental heat-transfer data indicate that an increasing angle of yaw can induce transition from laminar to turbulent boundary layer.

PUBLISHED JULY 1962

U. S. NAVAL ORDNANCE LABORATORY  
WHITE OAK, MARYLAND

NOLTR 62-35

8 June 1962

**Supersonic Aerodynamic Heat Transfer and Pressure Distribution  
on a Sphere-Cone Model at High Angles of Yaw**

This report represents the experimental phase of a project undertaken at NOL to obtain a more complete understanding of the heat transfer to blunt re-entry type bodies at angles of yaw. Measurements of the surface pressures and heat transfer to a yawed sphere-cone model in supersonic air flow have been made, and the data are compared with several theories.

This work was sponsored by the Bureau of Naval Weapons under Task No. RMGA-42-034/212-1/F009-10-001.

The author is indebted to Mr. S. M. Hastings for his stimulating comments and recommendations. He also wishes to acknowledge the valuable assistance of Mr. R. Chatham in making heat-transfer calculations, Mr. J. A. Iandolo in the mechanical design of the sting and roll mechanism, Mr. R. C. Sullivan in instrumenting and installing the model, and Mr. J. M. Kendall and Mr. G. W. Payne in building the related equipment for measuring temperatures.

W. D. COLEMAN  
Captain, USN  
Commander

FLORIAN GEINEDER  
By direction

NOLTR 62-35

CONTENTS

	Page
Introduction . . . . .	1
Experimental Testing Equipment . . . . .	1
Test Facility . . . . .	1
Description of Model . . . . .	1
Instrumentation . . . . .	2
Experimental Procedure . . . . .	3
Pressure Data . . . . .	3
Temperature Data . . . . .	3
Results and Discussion . . . . .	3
Pressure Results . . . . .	3
Temperature Results . . . . .	4
Heat-Transfer Data Reduction . . . . .	5
Heat-Transfer Results . . . . .	6
Conclusions . . . . .	8
References . . . . .	10

ILLUSTRATIONS

- Figure 1** Sphere-Cone Model Showing the Location of Pressure Orifices and Thermojunctions
- Figure 2** Schematic Diagram of Test Setup
- Figure 3** Schematic Diagram of Thermocouple Wiring
- Figure 4** Surface Pressure Distribution over the Sphere-Cone Model at  $M = 3.23$ ,  $\alpha = 6^\circ$
- Figure 5** Surface Pressure Distribution over the Sphere-Cone Model at  $M = 3.23$ ,  $\alpha = 18^\circ$
- Figure 6** Surface Pressure Distribution over the Sphere-Cone Model at  $M = 4.83$ ,  $\alpha = 6^\circ$
- Figure 7** Surface Pressure Distribution over the Sphere-Cone Model at  $M = 4.83$ ,  $\alpha = 18^\circ$
- Figure 8** Comparison Between the  $M = 3.23$  and  $M = 4.83$  Surface Pressure Distribution over the Sphere-Cone Model at  $\alpha = 18^\circ$
- Figure 9** The Measured Internal and External Wall Temperature Distributions on the Sphere-Cone Model at  $M = 4.83$ ,  $\alpha = 18^\circ$ , and  $\psi = 90^\circ$
- Figure 10** The Measured Internal and External Wall Temperature Distributions on the Sphere-Cone Model at  $M = 4.83$ ,  $\alpha = 18^\circ$ , and  $\psi = 90^\circ$
- Figure 11** The Measured Internal and External Wall Temperature Distributions on the Sphere-Cone Model at  $M = 4.83$ ,  $\alpha = 18^\circ$ , and  $\psi = 180^\circ$
- Figure 12** The Measured and Adjusted Internal and External Wall Temperature Distributions on the Sphere-Cone Model at  $M = 4.83$ ,  $\alpha = 18^\circ$ ,  $\psi = 0^\circ$  and  $180^\circ$
- Figure 13** Comparison Between Adjusted and Measured Temperatures on the Surface of the Sphere-Cone Model at  $M = 4.83$ ,  $\alpha = 18^\circ$ , and  $S/R = 0$  and  $0.52$
- Figure 14** Heat-Transfer Distribution to the Surface of a Sphere-Cone Model at  $M = 4.83$  and  $\alpha = 18^\circ$

- Figure 15** Heat-Transfer Distribution to the Surface of a Sphere-Cone Model at  $M = 3.23$  and  $\alpha = 18^\circ$
- Figure 16** Heat Transfer Versus Roll Angle for Constant Values of  $S/R = 0.301, 1.392$ , and  $2.636$  at  $M = 3.23$  and  $\alpha = 18^\circ$
- Figure 17** Heat Transfer Versus  $S/R$  for Constant Values of  $\psi = 60^\circ$  and  $75^\circ$  at  $M = 3.23$  and  $\alpha = 18^\circ$
- Figure 18** The Regions of Laminar, Transitional, and Turbulent Boundary Layers at  $M = 3.23$ ,  $\alpha = 18^\circ$

**TABLES**

- Table 1** Thermojunction and Pressure Orifice Locations
- Table 2** Pressure Distributions
- Table 3** Temperature Distribution Through Model Wall
- Table 4** Heat-Transfer Distribution

## SYMBOLS

$C_p$	local pressure coefficient
$C_{p_{\max}}$	stagnation point pressure coefficient
$c_p$	specific heat at constant pressure
$H$	enthalpy
$k$	thermal conductivity
$M$	Mach number
$n$	coordinate normal to model surface
$Nu$	Nusselt number, $Q c p_o r / k_{oe} (H_{oe} - H_w)$
$p$	local static pressure
$p'_o$	stagnation point pressure
$Q$	local heat-transfer rate
$R$	model base radius
$Re$	Reynolds number as given by $\frac{\rho_{oe} H_{oe}}{\mu_{oe}} r^{1/2}$
$Re_{\infty}$	free-stream Reynolds number per unit length as given by $\rho_{\infty} U_{\infty} / \mu_{\infty}$
$s$	distance along a meridian on the surface of the model measured from the point where the axis of symmetry intersects the surface of the spherical nose
$T$	local static temperature
$t$	time
$U_{\infty}$	free-stream velocity
$w$	velocity in the roll direction
$\alpha$	angle of yaw
$\eta$	an angle that describes the inclination of the model surface to the free-stream flow and is the angle between the free-stream velocity vector and the line normal to the surface

$\mu$  viscosity  
 $\rho$  density  
 $\psi$  roll angle

Subscripts

ADJ adjusted  
MEAS measured  
 $o$  stagnation conditions  
 $o_e$  local stagnation conditions at the outer edge of  
the boundary layer  
 $w$  the external surface of the model  
 $\infty$  free stream

## INTRODUCTION

High-speed missiles such as ballistic missile re-entry bodies, maneuverable interceptor missiles, and hypersonic glide vehicles are apt to fly at angles of yaw; therefore, it is necessary for the missile designer to be able to estimate the effect of the angle of yaw on the aerodynamic heat transfer to these missiles.

This report represents the experimental phase of a project undertaken at the Naval Ordnance Laboratory to achieve a better understanding of the problem of heat transfer to bodies at angles of yaw. Surface pressure and heat transfer data are presented for a sphere-cone model exposed to a supersonic air stream at angles of yaw. The heat-transfer data are obtained by measuring the steady-state temperatures on the boundaries of the model shell and solving the steady-state three-dimensional heat conduction equation utilizing an iteration process. Some comparisons are made between the experimental and theoretical heat-transfer data on the most windward and leeward streamlines of the model. Additional calculations along the streamlines will be made and the results will be presented in a future report.

The sphere-cone model used for this experimental investigation has been used previously to obtain heat-transfer data at  $M = 3.23$ ,  $\alpha = 0^\circ$ , and  $M = 4.83$ ,  $\alpha = 0^\circ$  and  $6^\circ$ , and the data are reported in reference (1).

## EXPERIMENTAL TESTING EQUIPMENT

Test Facility

Both the heat transfer and pressure measurements were made in the NOL Supersonic Wind Tunnel No. 2 which is described in reference (2). The supply conditions of the test are listed in the following table.

$M$	$T_o$	$P_o$	$Re_{\infty}$
3.23	318°K	980 mm Hg	$2.43 \times 10^6 \text{ ft}^{-1}$
4.83	320°K	2090 mm Hg	$2.50 \times 10^6 \text{ ft}^{-1}$

Description of Model

The sphere-cone model is made from type 347 stainless steel. It is instrumented with 60 stainless steel-constantan thermojunctions and each thermojunction is formed by welding

constantan wire of 0.005-inch diameter to the model wall. As shown in figure 1, the thermojunctions and pressure taps lie in the same meridian plane. The 11 pressure taps are located on one side of the axis of symmetry and the thermojunctions are located on the other side. The thermojunctions are located on both the inside and outside surfaces of the model wall. Table 1 gives the S/R values of both the thermojunctions and pressure taps. A more complete description of the construction of the sphere-cone model can be found in reference (1).

#### Instrumentation

A schematic diagram of the test setup is shown in figure 2. Continuous traces of  $p/p_0$  versus roll angle are recorded for one surface pressure tap at a time on a Kendall pressure ratio recorder which is described in reference (3). The surface pressure and supply pressure could also be read independently on a Wallace and Tiernan mercury manometer and Wallace and Tiernan pressure gage, respectively, in order to check the pressure ratio recorder.

The roll angle is recorded on the pressure ratio recorder and also displayed on the console of a self-balancing potentiometer which is a single channel of ADAPS (ref. (4)). The ADAPS is essentially a self-balancing potentiometer that balances the voltage drop across a variable resistor. The variable resistor is mounted on the model support and is geared to the rolling motion of the model. The rolling motion of the model is transmitted to the pressure ratio recorder by mounting a servo-transmitter on the ADAPS. The servo-transmitter is geared to the drive shaft of ADAPS and it sends an electrical signal to a servo-receiver on the pressure ratio recorder and to the visual readout.

Cooling of the sphere-cone model is achieved by circulating DC 200 silicone oil through the inside of the model. The silicone oil is passed through a coiled tube of a heat exchanger, the coil being immersed in a solid carbon dioxide-alcohol bath. A Taylor temperature controller keeps the silicone oil at a constant temperature of  $223^{\circ}\text{K} \pm 0.5^{\circ}\text{K}$ . The temperature of the silicone oil is  $230^{\circ}\text{K} \pm .5^{\circ}\text{K}$  as it enters the model, and is  $235^{\circ}\text{K} \pm .5^{\circ}\text{K}$  as it leaves the model. These temperatures are continually monitored on two General Electric millivolt recorders.

The output of each of the thermocouples is measured with a single channel of PADRE (ref. (5)), which is a self-balancing potentiometer. The potentiometer is set to a full-scale reading of 1 MV, thereby giving a voltage sensitivity of  $\pm 0.6 \mu\text{V}$  and a temperature sensitivity of  $\pm 0.02^{\circ}\text{K}$ . The

thermocouples are automatically switched one at a time to the potentiometer.

As shown in figure 3, the thermocouples on the outside surface of the model use an ice-water bath as a reference. The thermocouples on the inside surface and in the model wall, at a given S/R station, use the temperature on the outside surface at that S/R station as a reference. Because temperature differences exist that give a voltage greater than 1 MV, it is necessary to provide a millivolt source to counteract any signals in excess of 1 MV.

#### EXPERIMENTAL PROCEDURE

##### Pressure Data

Each of the 11 surface pressure taps is connected one at a time to the pressure ratio recorder. A continuous trace of  $p/p_0'$  versus  $\psi$  is produced when the model is rolled from the most windward to the most leeward position. The rolling motion is stopped every  $15^\circ$ , and the surface pressure and supply pressure are read on a mercury manometer and pressure gage, respectively.

##### Temperature Data

The temperature distribution through the model wall is obtained in the following manner. With the supply conditions of the wind tunnel and the model coolant constant with respect to time, the model is placed at the initial roll position of  $\psi = 0^\circ$ . After the temperatures throughout the model wall reach their steady-state values, they are recorded. The model is then rotated to the next roll position and this procedure is repeated. Temperature measurements are made in the region  $0^\circ \leq \psi \leq 180^\circ$ , at increments of  $\Delta\psi = 15^\circ$ .

#### RESULTS AND DISCUSSION

##### Pressure Results

Pressure distributions on the sphere-cone model are presented in table 2. They are given in the dimensionless form  $p/p_0'$  versus S/R for various values of the roll angle  $\psi$  in increments of  $5^\circ$ .

Figures 4, 5, 6, and 7 are representative plots of  $p/p_0'$  versus S/R for  $\psi = 0^\circ$ ,  $90^\circ$ , and  $180^\circ$  at  $\alpha = 6^\circ$  and  $18^\circ$  at  $M = 3.23$  and  $4.83$ . The Newtonian flow ( $C_p/C_{p_{max}} = \cos^2\eta$ ) predicts a pressure distribution on the spherical nose that

is slightly higher than the experimental data. On the conical afterbody the pressures calculated from Newtonian flow and the Kopal cone tables (refs. (6), (7), and (8)) are slightly lower than the experimental data. Both the Newtonian and Kopal values predict a constant pressure as a function of S/R along the most windward and leeward streamlines of the cone section, whereas the experimental pressure distributions show a slight overexpansion in the region of the sphere-cone junction and then a slight compression to a constant pressure with increasing S/R.

For various values of S/R a cross plot of the pressure distributions, that is,  $p/p_0$  versus  $\psi$ , is shown in figure 8. The data for  $\alpha = 18^\circ$  at Mach numbers of 3.23 and 4.83 are presented. The experimental data are shown as they are recorded, that is, as continuous curves of pressure versus roll angle. The pressure level is slightly greater at  $M = 3.23$  than at  $M = 4.83$ .

#### Temperature Results

All of the measured temperature distributions are presented in table 3. They are given in degrees Kelvin versus S/R for various values of roll angle  $\psi$  in increments of  $15^\circ$ .

Figures 9, 10, and 11 are plots of the measured wall temperatures of the model, versus S/R, for  $\psi = 0^\circ$ ,  $90^\circ$ , and  $180^\circ$ , and with  $M = 4.83$  and  $\alpha = 18^\circ$ . Notice that the temperature on the surface of the spherical nose of the model at S/R = 0 varies almost  $3^\circ\text{C}$  as  $\psi$  goes from  $0^\circ$  to  $180^\circ$ . Under ideal conditions, that is, if tunnel supply conditions and the temperature of the coolant fluid inside the model remain constant, the temperature at the point S/R = 0 should remain constant because this point is on the axis of rotation of the spherical nose of the model and remains in the same position relative to the air flow. As can be seen in figure 12 the varying temperature at S/R = 0 gives a discontinuity in the temperature distribution at S/R = 0. It is likely that the discontinuity is caused by an asymmetry in the geometry of the model due to the presence of the pressure taps. In order to eliminate this discontinuity, the temperature at S/R = 0, for all roll positions of  $\psi > 0^\circ$ , is adjusted so that it is equal to the temperature at  $\psi = 0^\circ$ . Then the assumption is made that the entire temperature distribution at a constant roll position shifts by the same amount as the change in temperature at S/R = 0. The equation for the temperature adjustment is:

$$T_{ADJ}(\psi, S/R) = T_{MEAS}(0,0) - T_{MEAS}(\psi,0) + T_{MEAS}(\psi,S/R) \quad (1)$$

This alters the temperature distribution as a function of the roll angle, but does not change the temperature difference across the wall. The adjustments in temperature do not change the ratio  $T_w/T_0$  more than 5 percent. Figure 12 illustrates how the discontinuity in the temperature distribution is eliminated by the temperature adjustment. Figure 13 is a plot of temperature versus roll angle for  $M = 4.83$ ,  $\alpha = 18^\circ$ , and  $S/R = 0$  and 0.52. This figure illustrates how the temperature distribution in the roll direction is affected by the temperature adjustment.

#### Heat-Transfer Data Reduction

The calculation of the aerodynamic heat transfer is performed by utilizing the steady-state method. A detailed description of the steady-state method can be found in reference (9). In general, this method requires the solution of the three-dimensional, steady-state heat conduction equation. Specifically for this problem, the shell of the model is separated into two regions. The first region is the spherical section and the second region is the conical section. The three-dimensional steady-state heat conduction equation is written in spherical and rectangular coordinate systems for the first and second regions, respectively. Then the heat conduction equation is replaced by a set of finite difference equations and the steady-state adjusted temperatures on the boundaries of the model shell are used to compute the temperature within the model shell utilizing an iteration process. The calculated temperature field is then used to find the temperature gradient normal to the model surface, and the local aerodynamic heat transfer to the model surface is:

$$Q = k \frac{\partial T}{\partial n} . \quad (2)$$

The variation of the thermal conductivity of the stainless-steel model as a function of temperature has been measured by the National Bureau of Standards and the results are presented in reference (10). In the temperature region,

$$223^\circ\text{K} \leq T \leq 273^\circ\text{K}$$

the thermal conductivity can be approximated by

$$k = (6.354 \times 10^{-6}) T + (2.31 \times 10^{-3}) \quad (3)$$

where the units are:

$$T \quad ^\circ\text{K}$$

$$k \quad \text{BTU/sec-ft-}^\circ\text{K} .$$

Heat-Transfer Results

Heat-transfer results are given in the form of the Nusselt number divided by the square root of the Reynolds number as suggested in reference (11) and the equation is:

$$\frac{Nu}{Re^{1/2}} = \frac{Qc_{p_0} r/k_{o_e} (H_{o_e} - H_w)}{(\rho_{o_e} H_{o_e} r/\mu_{o_e})^{1/2}} . \quad (4)$$

If  $c_p$  = constant ( $c_p$  varies about 0.3 percent in the temperature range encountered in this experiment) and if the local stagnation density, pressure, and enthalpy are constant about the body, then equation (4) can be written in the form:

$$Nu/Re^{1/2} = (\text{constant}) \frac{Q}{T_o - T_w} \quad (5)$$

where

$$(\text{constant}) = \frac{r/k_{o_e}}{(\rho_{o_e} H_{o_e} r/\mu_{o_e})^{1/2}} . \quad (6)$$

Figure 14 is a plot of the heat-transfer data versus S/R for  $M = 4.83$ ,  $\alpha = 18^\circ$ , and  $\psi = 0^\circ$ ,  $90^\circ$ , and  $180^\circ$ .

Theoretical calculations of the laminar heat transfer have been made for both the windward ( $\psi = 0^\circ$ ) and leeward ( $\psi = 180^\circ$ ) streamlines and the results are shown in figure 14. On the windward streamline ( $\psi = 0^\circ$ ), the analysis of Vaglio-Laurin (ref. (12)) as formulated by Zakkay (ref. (11)) is used to compute the heat transfer downstream from the aerodynamic stagnation point. Using this method two calculations are made. The first calculation is made under the assumption that the heat transfer on the windward streamline is equivalent to that on an axially symmetric sphere-cone body which has a new cone half angle of the actual body plus the angle of yaw. In the second calculation, the effect of the crosswise velocity gradient  $dw/d\psi$  on the spreading of the streamlines of the inviscid flow is approximately accounted for and the value of  $dw/d\psi$  is determined by using equations (1) and (A-22) of reference (11) and is assumed to be constant. The three constants in equation (1) of reference (11) are determined from the pressures that were measured at a constant  $S/R = 2.481$ , and  $\psi = 0^\circ$ ,  $90^\circ$ , and  $180^\circ$ . Both calculations give the same heat-transfer values on the spherical nose of the body and these values are from 0 percent to 13 percent higher than experimental data. On the conical section of the body the former calculation compares favorably with the experimental data, as may be seen from figure 14, while the latter calculation predicts heat-transfer values that are approximately 30 percent higher than the measured data.

Another theoretical heat-transfer curve using the method of Reshotko (ref. (13)) is also computed for the most windward streamline of the cone. Reshotko's analysis is for a sharp cone at an angle of yaw and as might be expected, the theoretical results seem to approach the measured heat-transfer values toward the base of the cone.

Since the measured static pressure distribution is relatively constant for  $\psi$  between  $135^\circ$  and  $180^\circ$  on the conical section of the model, a calculation of the laminar heat transfer was made using flat-plate theory, and the results were transformed to the cone geometry by multiplying the flat-plate results by  $\sqrt{3}$ . This computation was made using the results of figure 6 of reference (14). The results agree favorably with the experimental data.

The heat transfer versus S/R for  $M = 3.23$ ,  $\alpha = 18^\circ$ , and  $\psi = 0^\circ$ ,  $90^\circ$ , and  $180^\circ$  is shown in figure 15. Theoretical calculations of the heat transfer using the same methods described in the previous paragraph are also shown in figure 15. When the heat-transfer rates are presented in the form of  $Nu/Re^{1/2}$ , the experimental and theoretical laminar heat-transfer distributions do not change very much between  $M = 3.23$  and  $M = 4.83$ . In figure 15, there is a sharp increase in the heat-transfer rates on the  $\psi = 90^\circ$  and  $180^\circ$  curves, indicating that a transition from laminar to turbulent flow has taken place. Theoretical values of the turbulent heat transfer to the leeward streamline have been obtained by transforming the flat-plate theoretical results of reference (14) so that they apply for a sharp cone. The theoretical results compare very well with the experimental data.

It is interesting to note that the experimental data in figure 15 indicate that there is no transition from laminar to turbulent boundary layer on the most windward streamline ( $\psi = 0^\circ$ ).

In order to illustrate where transition begins, figures 16 and 17 are presented. Figure 16 is a plot of the experimental heat-transfer parameter  $Nu/Re^{1/2}$  versus  $\psi$  with S/R as a parameter. Values for S/R equal to 0.301, 1.392, and 2.636 are shown. The first two curves indicate that the heat-transfer rates decrease as  $\psi$  increases, whereas, the third curve shows that there is a sharp rise in the heat-transfer rates at  $\psi = 75^\circ$ . In figure 17, the experimental  $Nu/Re^{1/2}$  is plotted against S/R and the  $\psi = 60^\circ$  data are completely laminar, however, the  $\psi = 75^\circ$  data show a sharp increase in the heat-transfer rates. The location of the laminar, transitional, and turbulent boundary layers on the conical section of the sphere-cone model are shown in figure 18. These regions are determined from the experimental

heat-transfer data. The point where the heat-transfer rates begin to rise is taken as the end of the laminar region and the point where the heat-transfer values reach a maximum is taken as the end of the transition region.

The region where transition begins is one where a true three-dimensional boundary layer with crossflow (that is, flow in the boundary layer normal to the external inviscid streamlines) does exist. Experiments having to do with flow on a rotating disk (ref. (15)) verify that a three-dimensional laminar boundary layer is extremely unstable. The Reynolds number based on local flow conditions and distance from the aerodynamic stagnation point to the base of the cone on the most windward streamline is  $1.4 \times 10^6$ , and there is no indication of transition. The Reynolds number at the beginning of transition at the point  $S/R = 1.6$  and  $\gamma = 90^\circ$  is only  $0.7 \times 10^6$ .

#### CONCLUSIONS

Newtonian flow theory predicts pressures on the surface of the spherical nose of the sphere-cone model that are slightly higher than the experimental data. The surface pressures given by the Kopal cone tables are slightly higher than those measured on the surface of the cone. Neither computational method is adequate for predicting the pressures in the region of the sphere-cone junction.

The theoretical laminar heat-transfer distributions along the windward streamline approach the experimental data toward the base of the cone. In the region of the sphere-cone junction the theoretical laminar heat-transfer rates are over 100 percent higher than the experimental measurements. The prediction of both the laminar and turbulent heat-transfer rates to the leeward streamline are in very good agreement with the experimental data.

The experimental laminar heat-transfer distributions are very nearly the same for both the Mach number 3.23 and 4.83 data, when they are expressed in the form of the Nusselt number divided by the square root of the Reynolds number.

The Mach number 3.23 experimental heat-transfer data indicate that increasing angles of yaw can cause transition from a laminar to a turbulent boundary layer in a region on the conical section of the model between the most windward and leeward streamlines. The experimental turbulent heat-transfer at a point on the cone that is midway between the most windward and leeward streamlines are approximately 50 percent higher than the experimental laminar heat transfer at the most

NOLTR 62-35

windward streamline. This transition is probably due to the extreme instability of the three-dimensional laminar boundary layer that exists in this region.

## REFERENCES

- (1) Hastings, S. M. and Chones, A. J., "Supersonic Aerodynamic Heating of a Yawed Sphere-Cone Wind-Tunnel Model," NAVORD Report 6812, 28 June 1960
- (2) Meek, P. P., "Aeroballistic Research Facilities," NOLR 1233, May 1959
- (3) Kendall, J. M., "Equipment for Continuously Recording the Ratio of Two Pressures," NAVORD Report 4201, September 1955
- (4) Gilbert, B. D., "Automatic Data Processing Systems (ADAPS) for the Supersonic Tunnels," NAVORD Report 2813, March 1953
- (5) Kendall, J. M., "Portable Automatic Data Recording Equipment (PADRE)," NAVORD Report 4207, 24 August 1959
- (6) Staff of the Computing Section, Center of Analysis, MIT, directed by Kopal, Z., "Tables of Supersonic Flow Around Cones," Technical Report No. 1, 1947
- (7) Staff of the Computing Section, Center of Analysis, MIT, directed by Kopal, Z., "Tables of Supersonic Flow Around Yawing Cones," Technical Report No. 3, 1947
- (8) Staff of the Computing Section, Center of Analysis, MIT, directed by Kopal, Z., "Tables of Supersonic Flow Around Cones of Large Yaw," Technical Report No. 5, 1949
- (9) Orlow, T. A., "Numerical Solution of LaPlace's Equation for Various Three Dimensional Regions with Axial Symmetry," NAVORD Report 6038, 22 January 1958
- (10) Robinson, H. E. and Watson, T. W., "Thermal Conductivity at Low Temperatures of Types 316 and 347 Stainless Steels," NBS Report 5748, January 1958
- (11) Zakkay, Victor, "Pressure and Laminar Heat Transfer Results in Three-Dimensional Hypersonic Flow," WADC TN-58-182, ASTIA Document No. 155679, September 1958
- (12) Vaglio-Laurin, Roberto, "Laminar Heat Transfer on Blunt-Nosed Bodies in Three-Dimensional Hypersonic Flow," WADC-TN-58-147, ASTIA Document No. AD 155588, May 1958
- (13) Reshotko, Eli, "Laminar Boundary Layer with Heat Transfer on a Cone at Angle of Attack in a Supersonic Stream," NACA TN-4152, December 1957
- (14) Van Driest, E. R., "The Problem of Aerodynamic Heating," Aeronautical Engineering Review, Vol. 15, No. 10, pp. 26-41, October 1956
- (15) Gregory, N., Stuart, J. T., and Walker, W. S., "On the Stability of Three-Dimensional Boundary Layer with Application to the Flow Due to a Rotating Disk," Paper No. 3 from the International Symposium on Boundary Layer Effects in Aerodynamics, held at the National Physical Laboratory, Teddington, England, 31 March and 1 April 1955, published by Philosophical Library, Inc., 1957

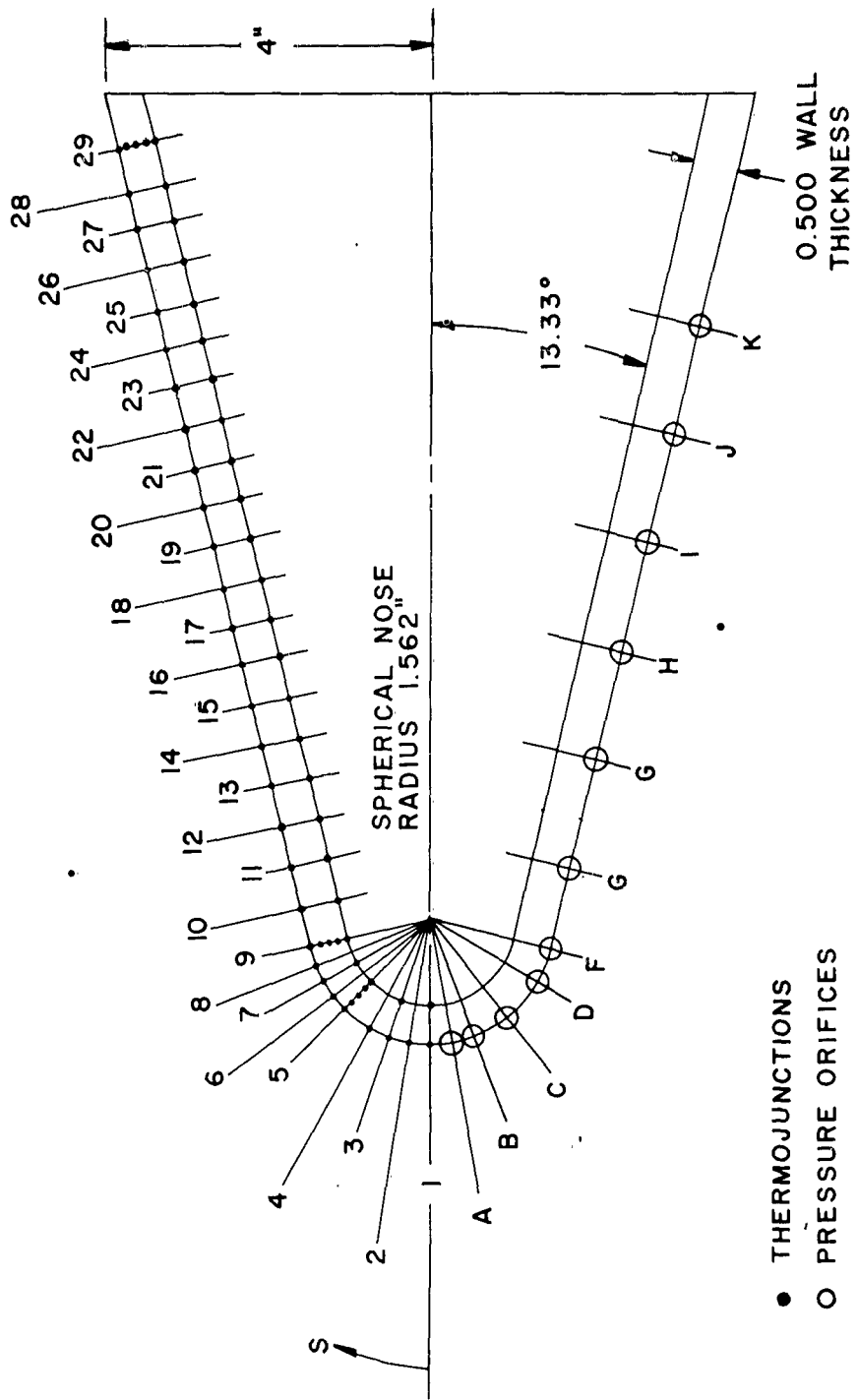


FIG. I SPHERE-CONE MODEL SHOWING THE LOCATION OF PRESSURE ORIFICES AND THERMOJUNCTIONS

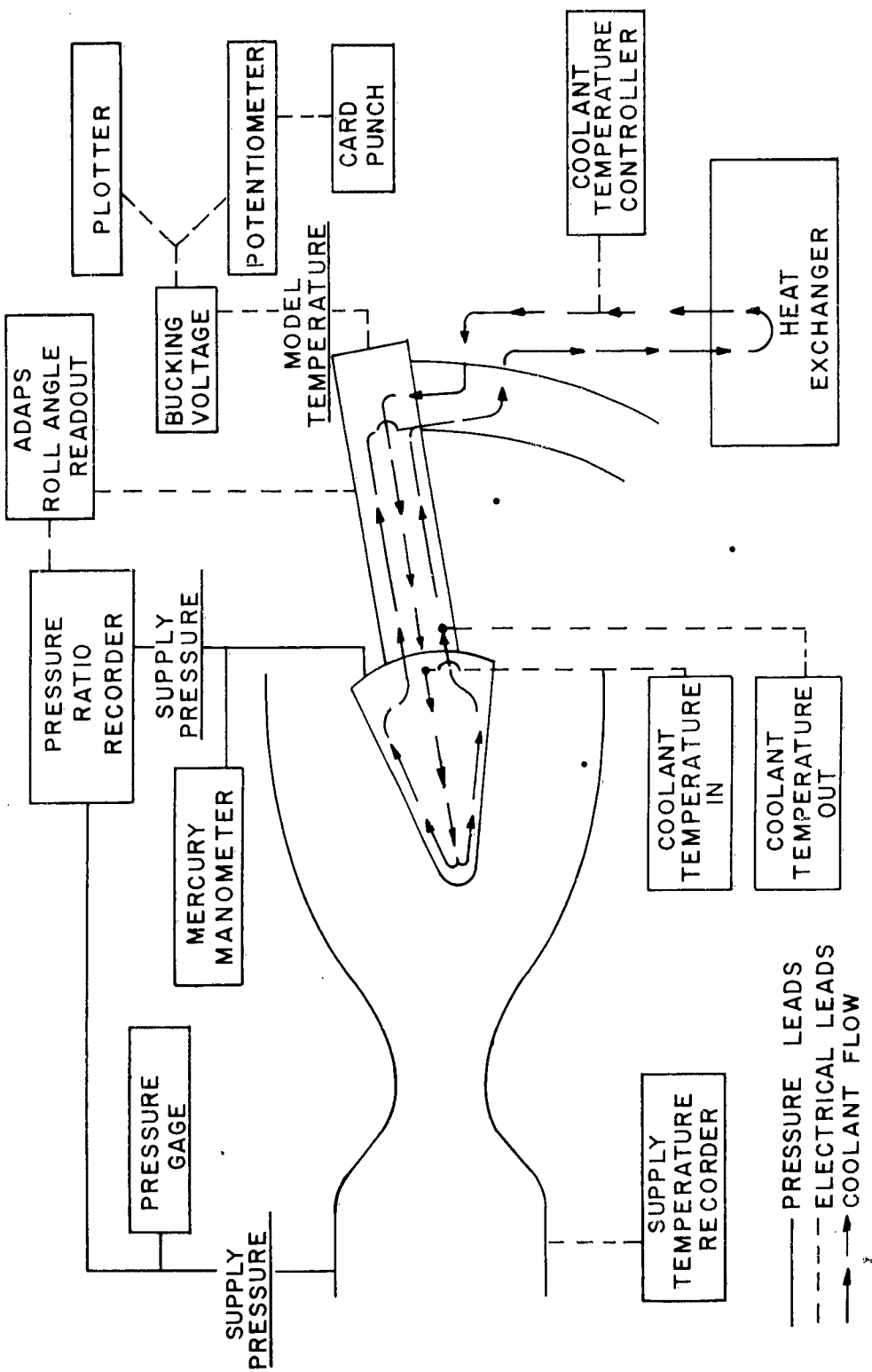


FIG 2 SCHEMATIC DIAGRAM OF THE TEST SETUP

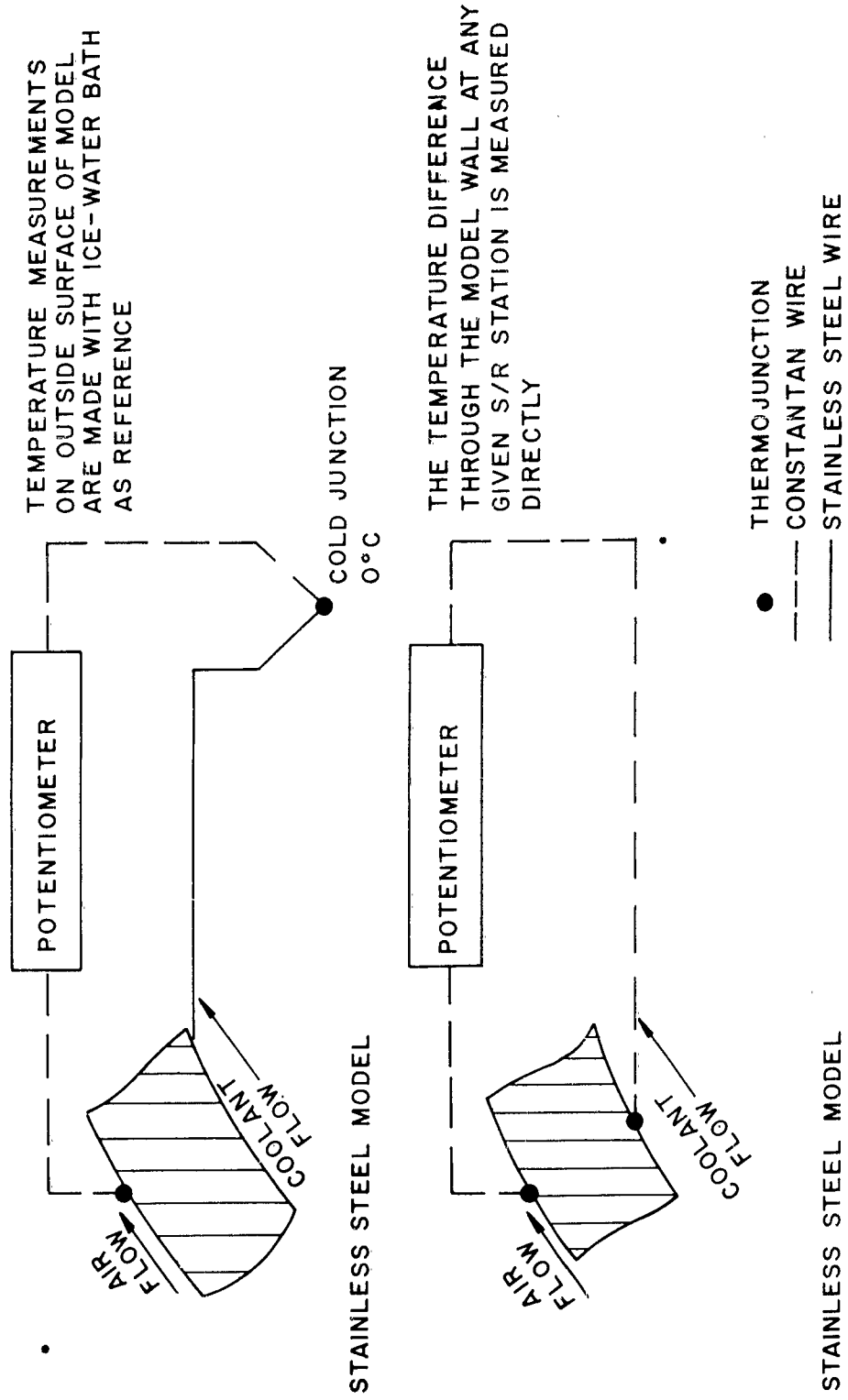


FIG. 3 SCHEMATIC DIAGRAM OF THERMOCOUPLE WIRING

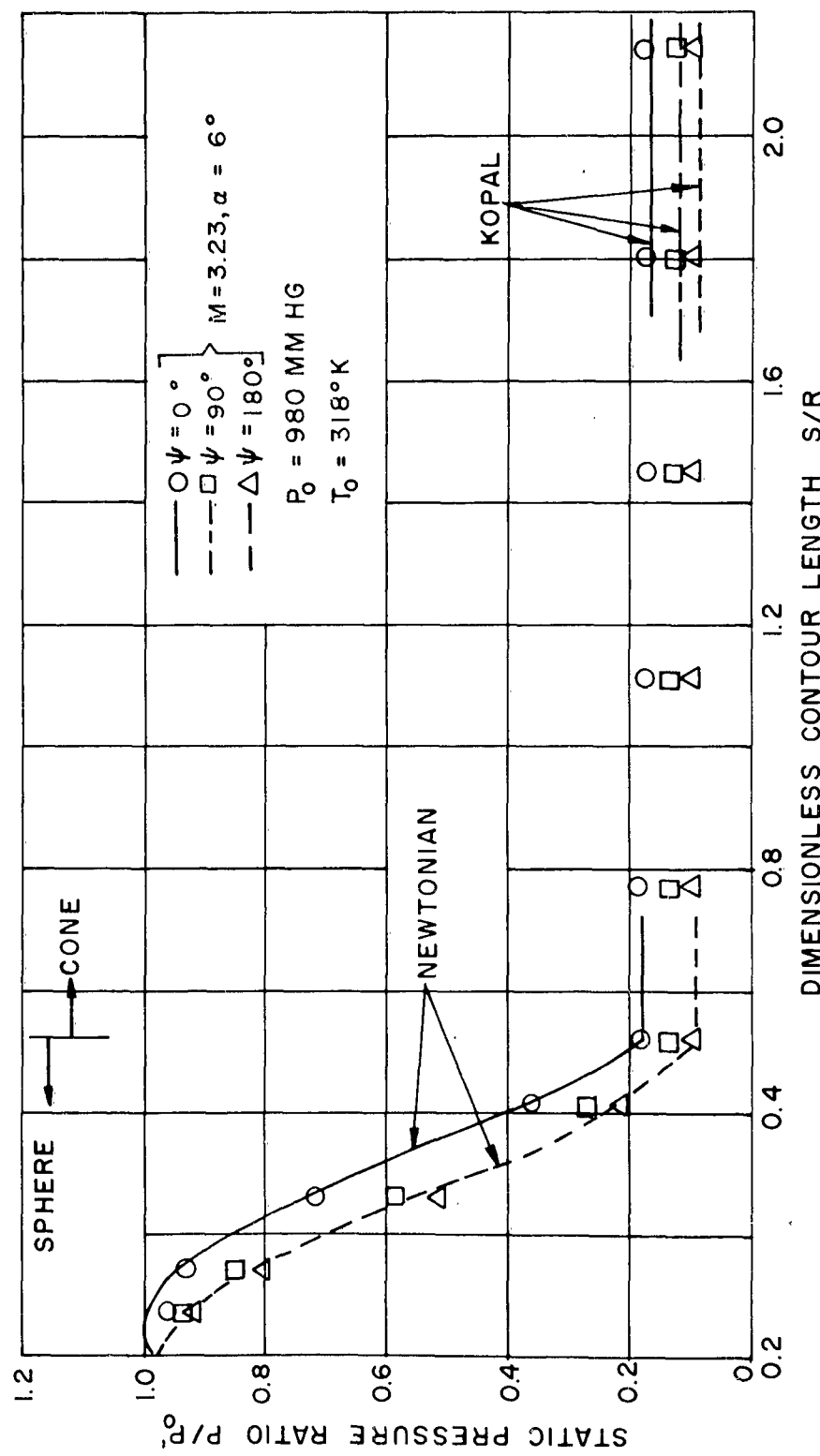


FIG. 4 SURFACE PRESSURE DISTRIBUTION OVER THE SPHERE-CONE  
MODEL AT  $M = 3.23, \alpha = 6^\circ$

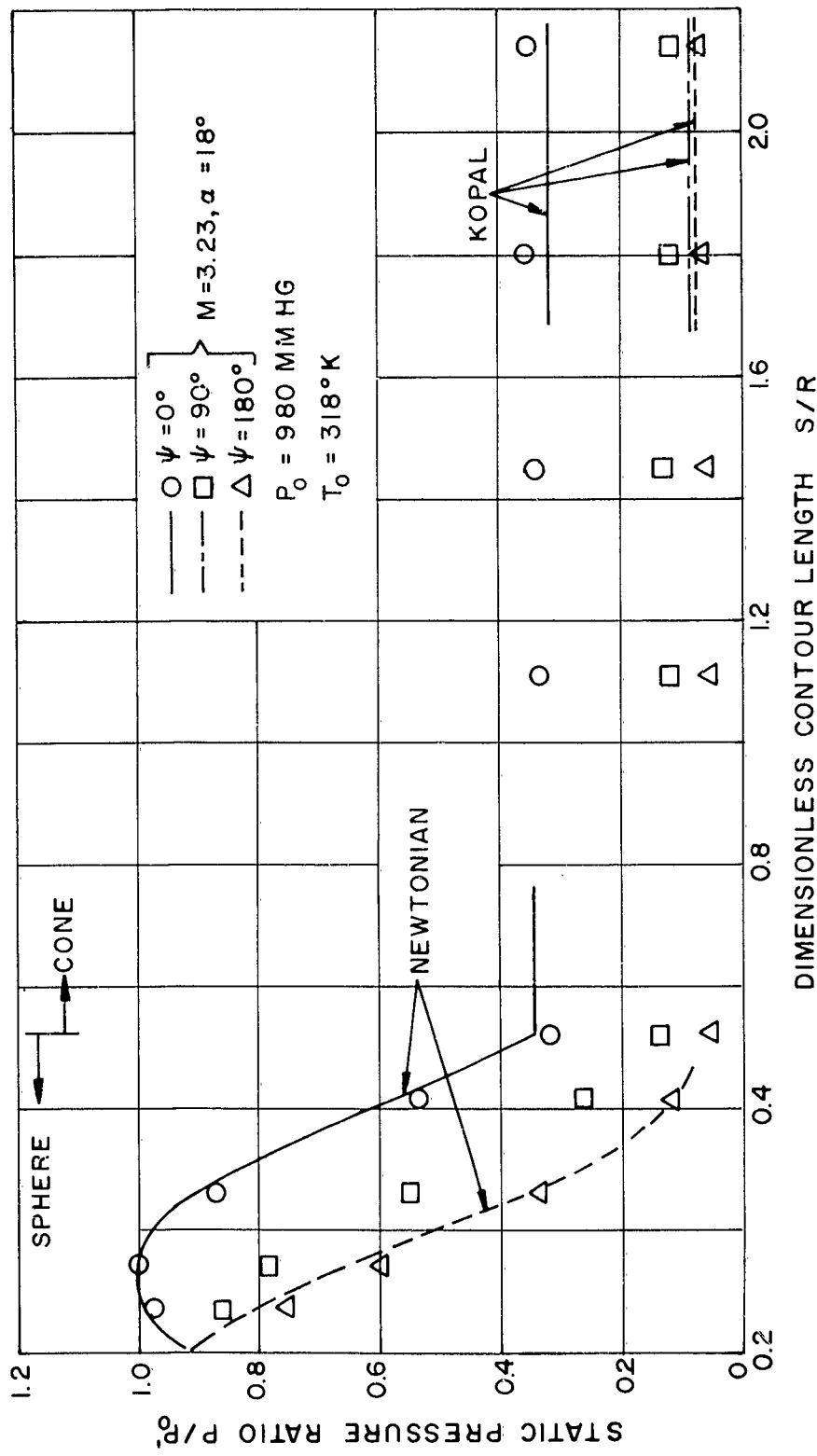


FIG. 5 SURFACE PRESSURE DISTRIBUTION OVER THE SPHERE-CONE  
MODEL AT  $M = 3.23, \alpha = 18^\circ$

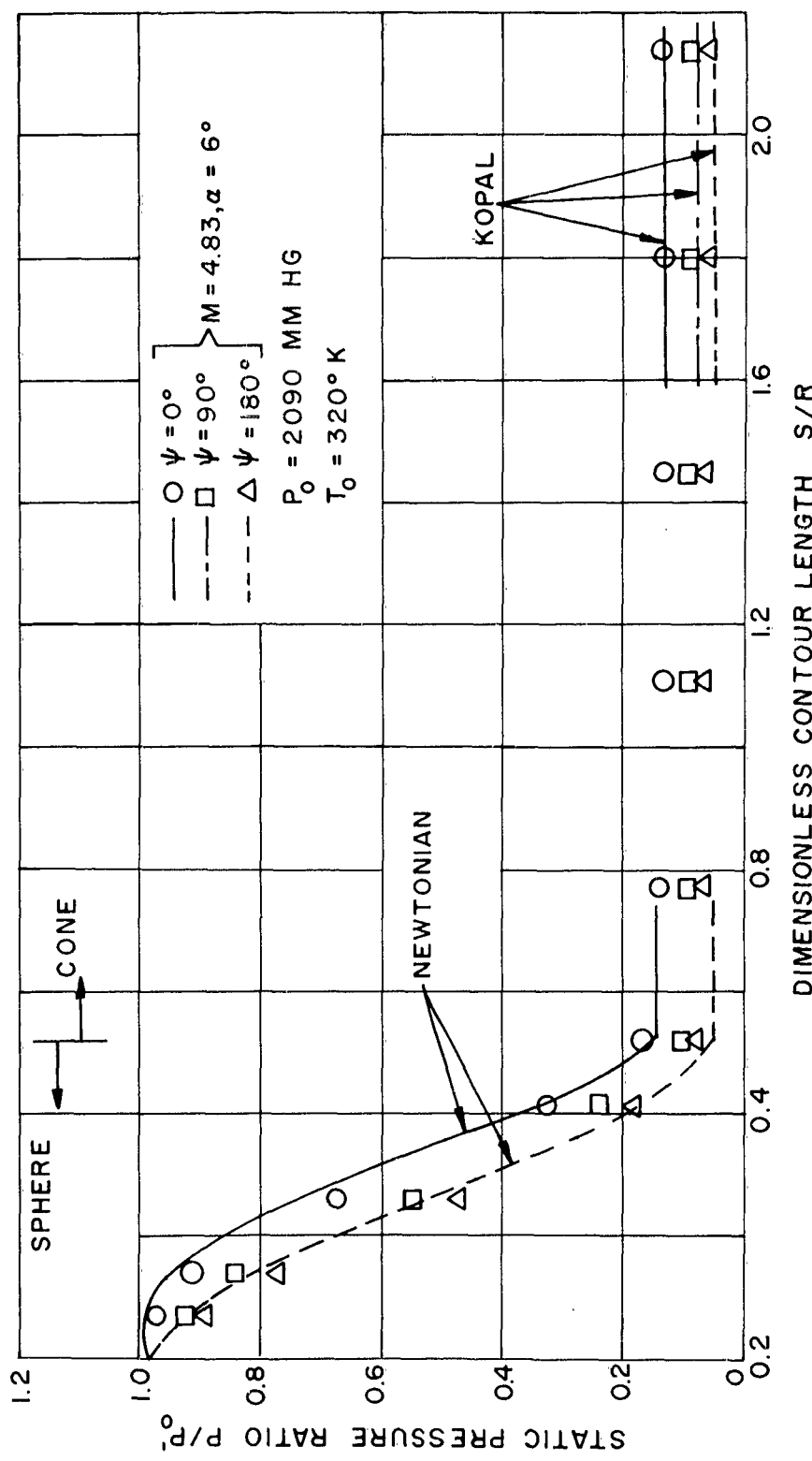


FIG. 6 SURFACE PRESSURE DISTRIBUTION OVER THE SPHERE-CONE MODEL AT  $M=4.83, \alpha=6^\circ$

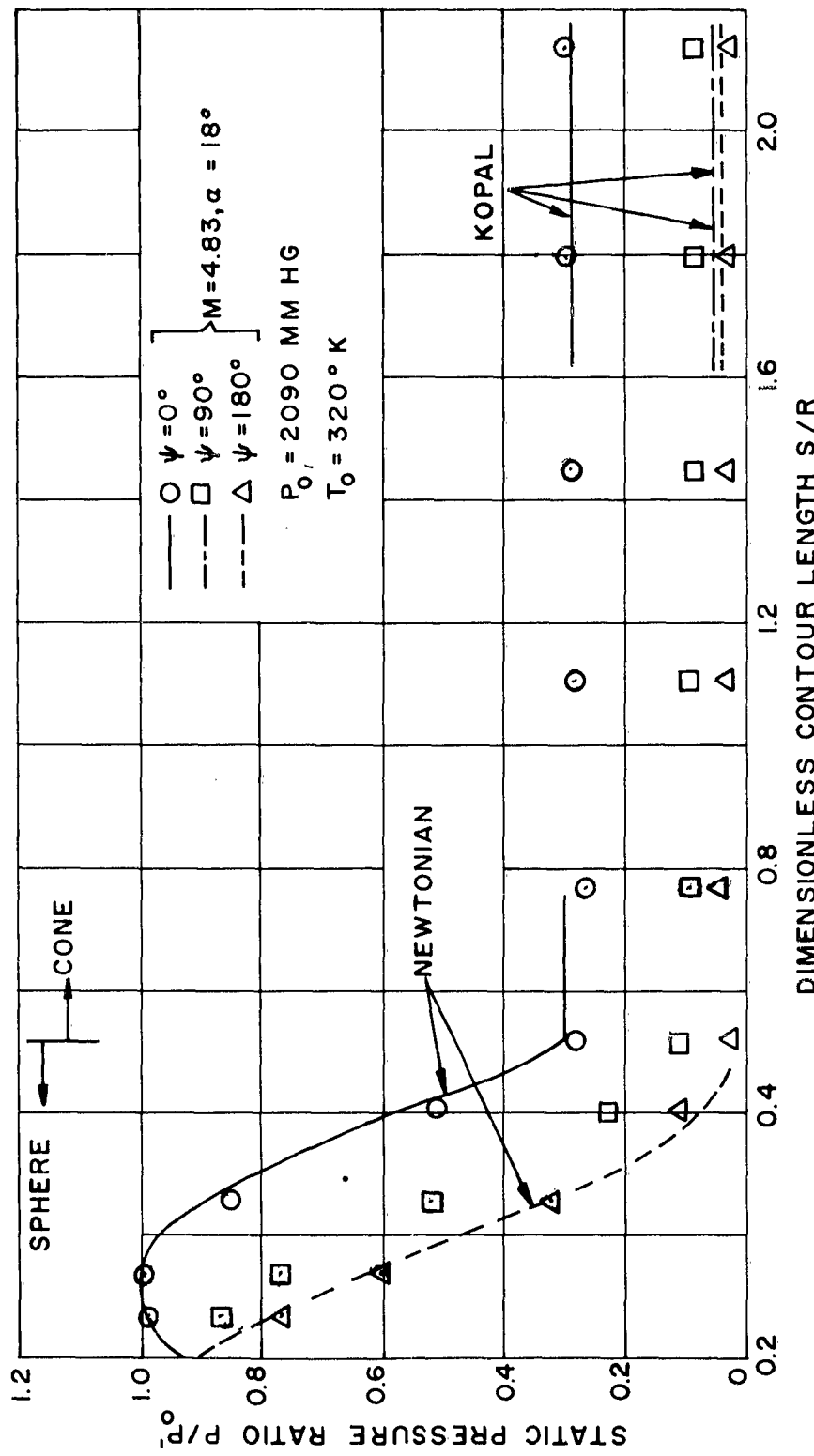


FIG. 7 SURFACE PRESSURE DISTRIBUTION OVER THE SPHERE-CONE  
MODEL AT  $M=4.83, \alpha = 18^\circ$

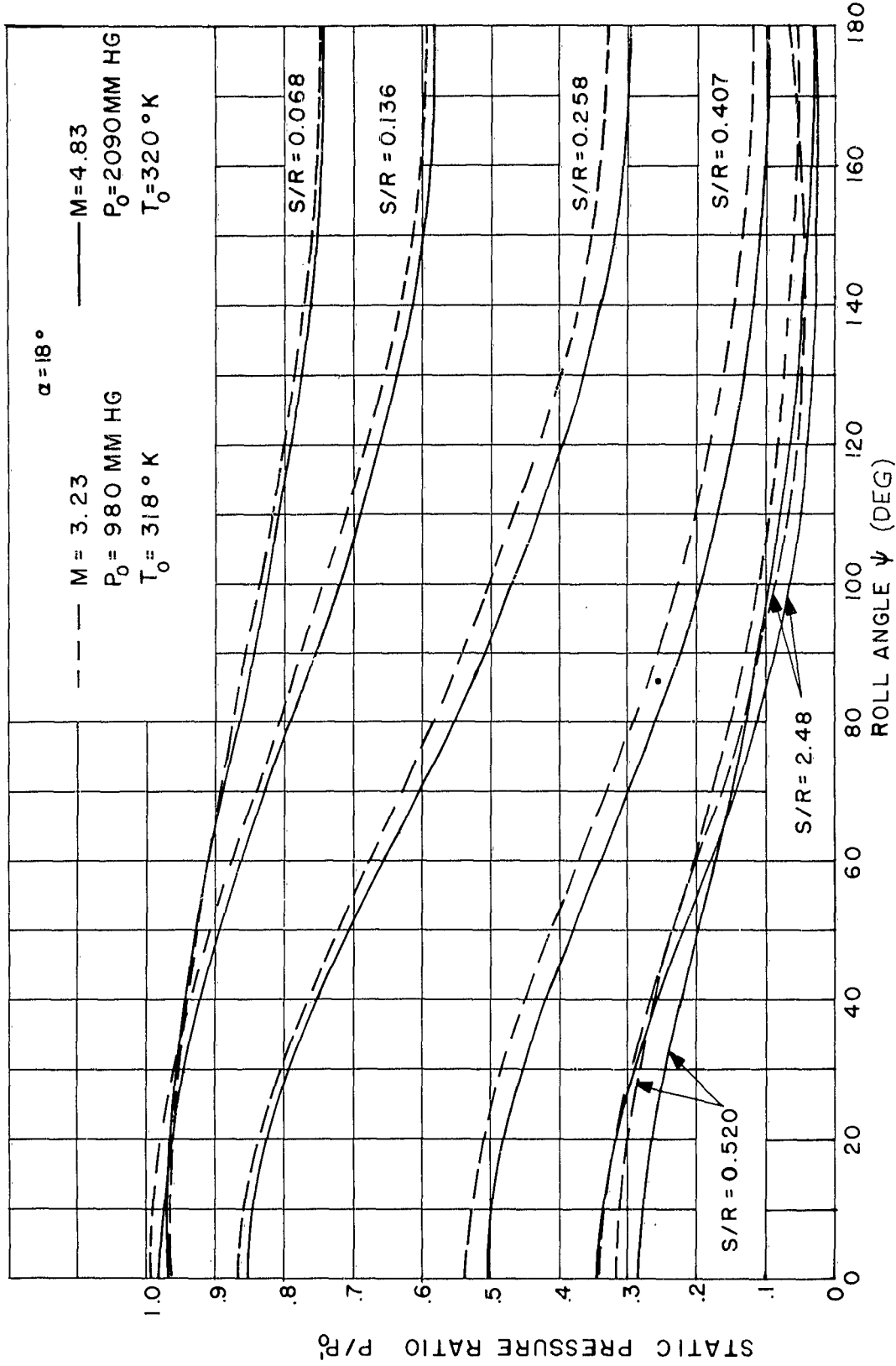


FIG. 8 COMPARISON BETWEEN THE M = 3.23 AND M = 4.83 SURFACE PRESSURE DISTRIBUTION OVER THE SPHERE-CONE MODEL AT  $\alpha = 18^\circ$

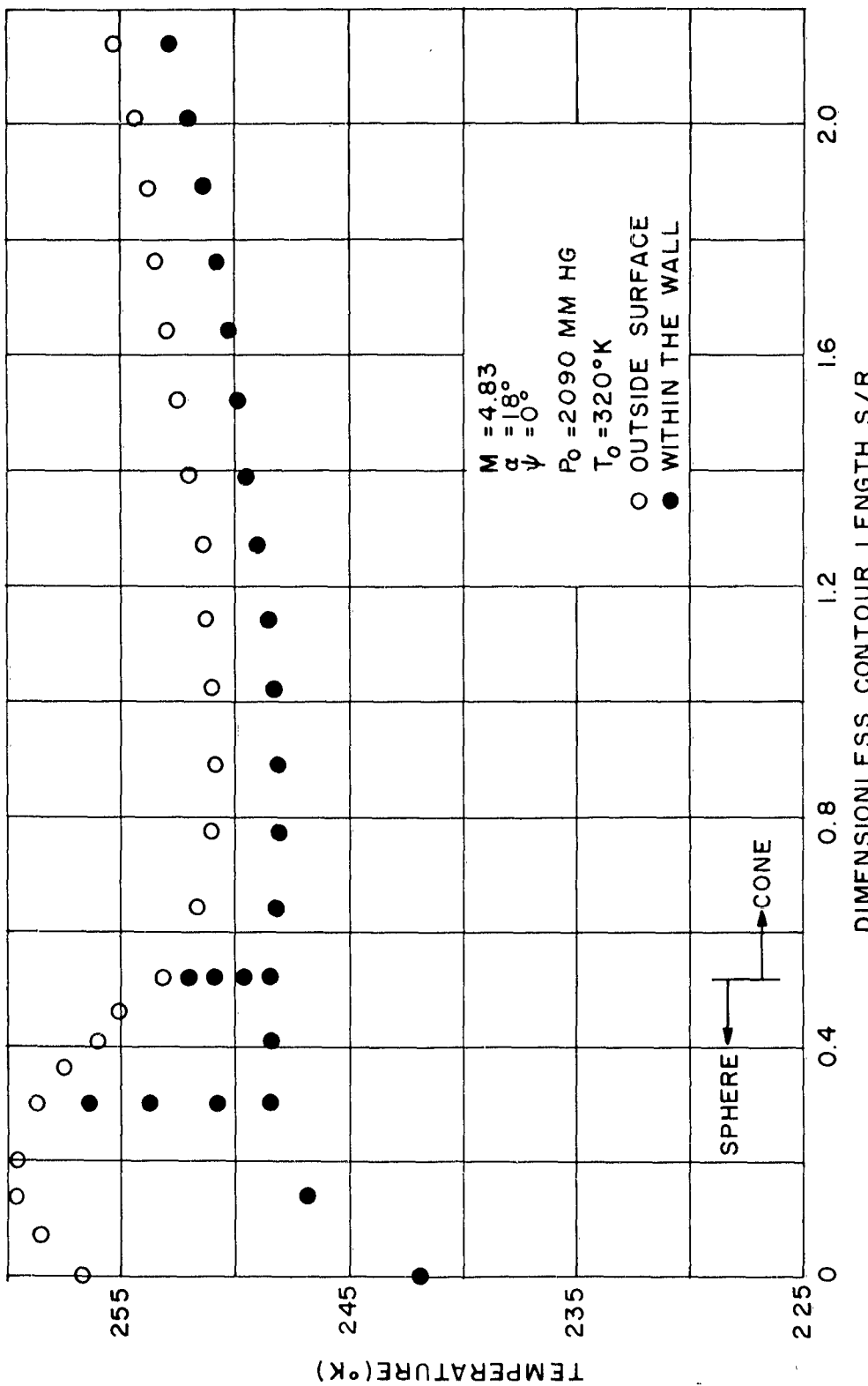


FIG. 9 THE MEASURED INTERNAL AND EXTERNAL WALL TEMPERATURE DISTRIBUTION ON THE SPHERE-CONE MODEL AT  $M = 4.83, \alpha = 18^\circ$  AND  $\psi = 0^\circ$ .

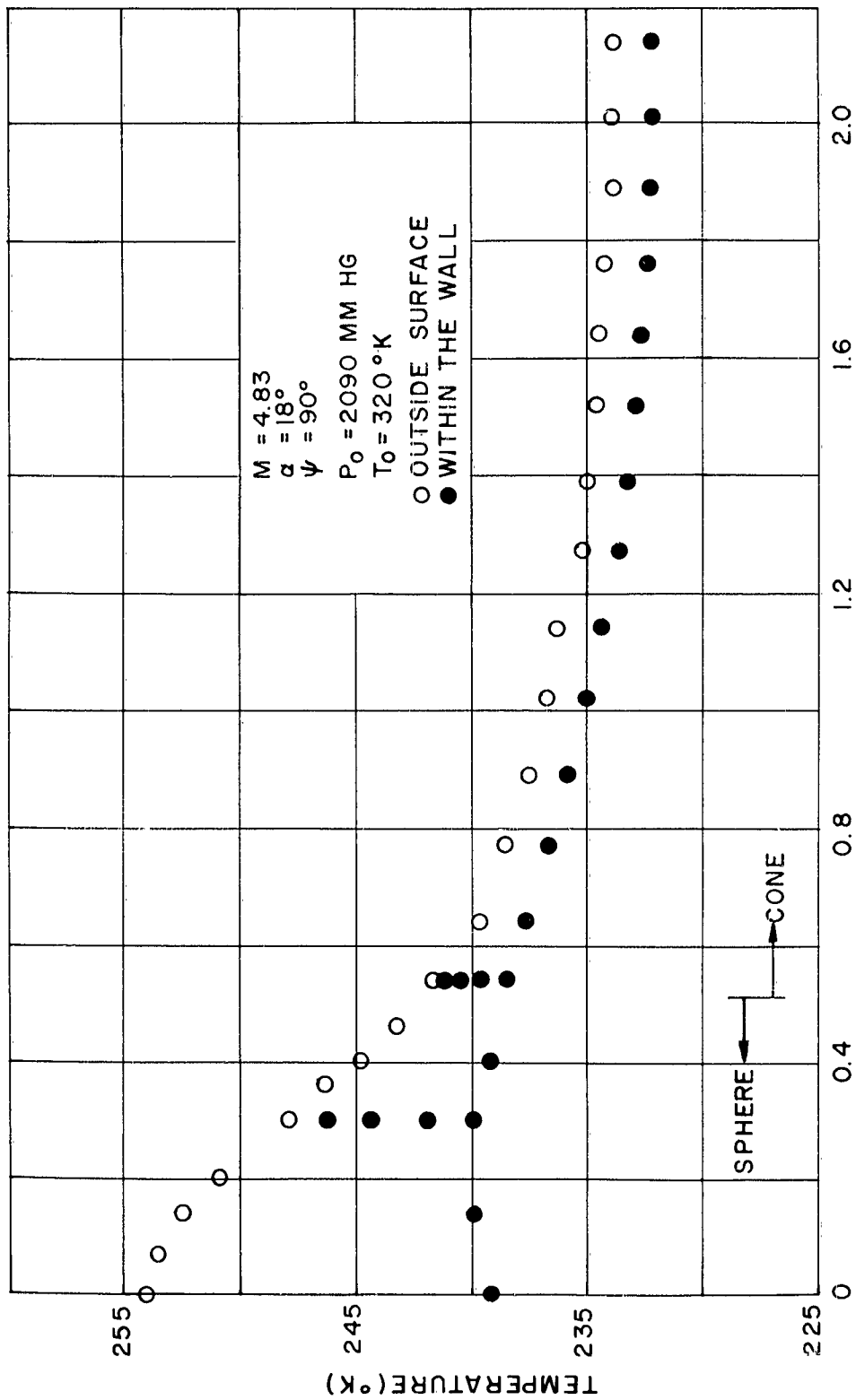


FIG. 10 THE MEASURED INTERNAL AND EXTERNAL WALL TEMPERATURE DISTRIBUTION ON THE SPHERE - CONE MODEL AT  $M = 4.83, \alpha = 18^\circ$  AND  $\psi = 90^\circ$

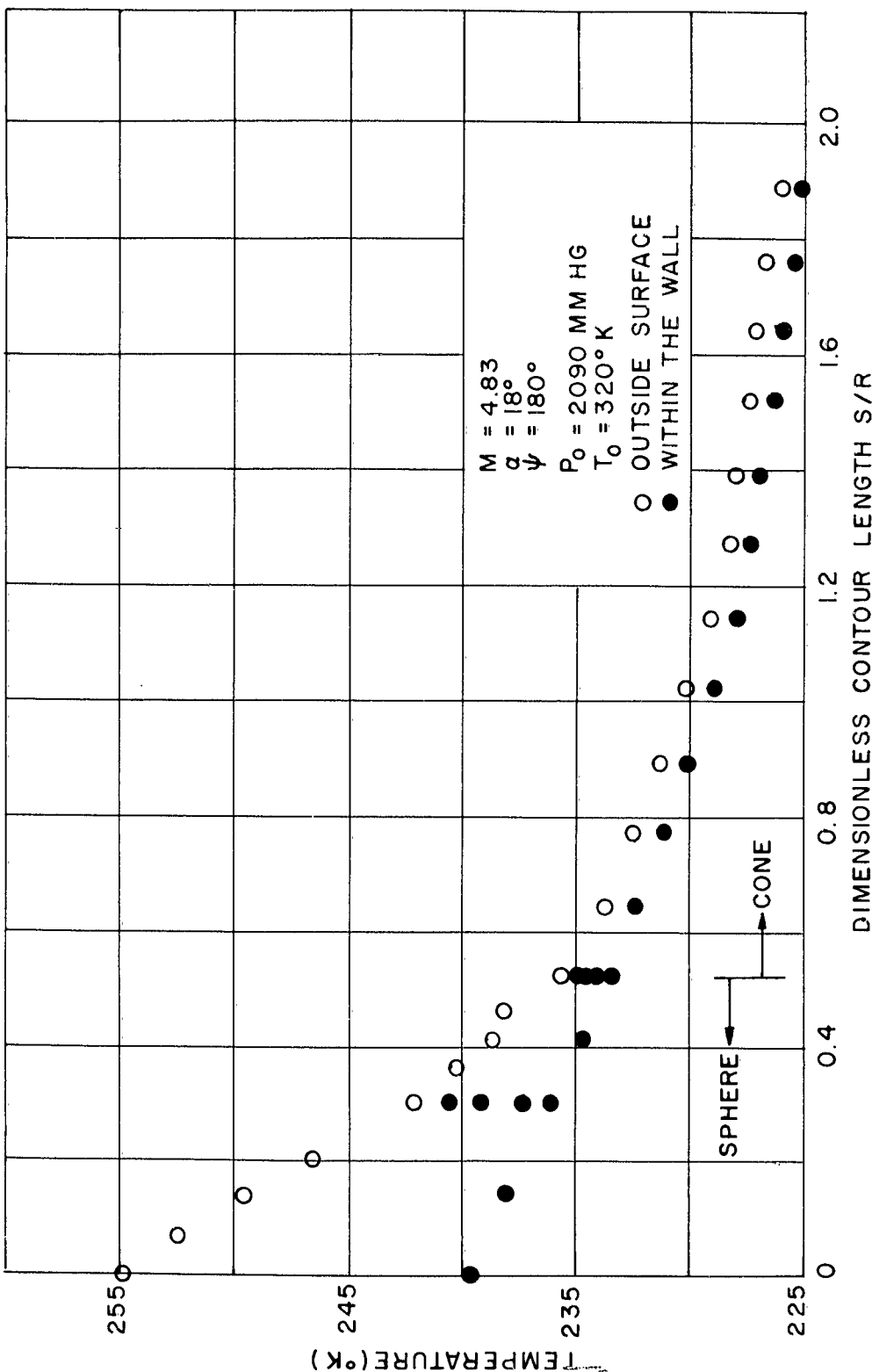


FIG. II THE MEASURED INTERNAL AND EXTERNAL WALL TEMPERATURE DISTRIBUTION ON THE SPHERE-CONE MODEL AT  $M = 4.83, \alpha = 18^\circ$  AND  $\psi = 180^\circ$

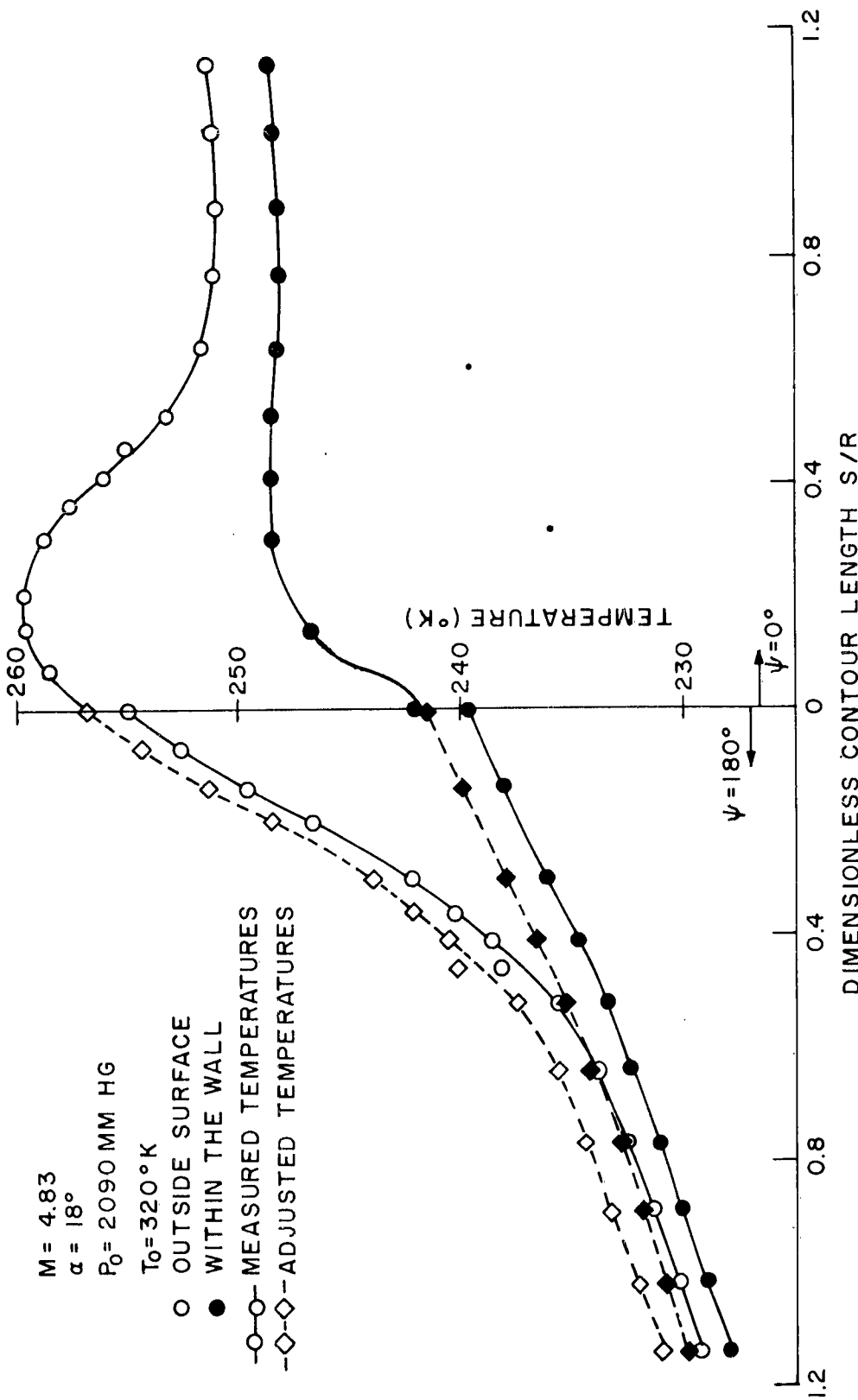


FIG. 12 THE MEASURED AND ADJUSTED INTERNAL AND EXTERNAL WALL TEMPERATURE DISTRIBUTIONS ON THE SPHERE-CONE MODEL AT  $M = 4.83$ ,  $\alpha = 18^{\circ}$ , AND  $\psi = 0^{\circ}$ , AND  $180^{\circ}$ .

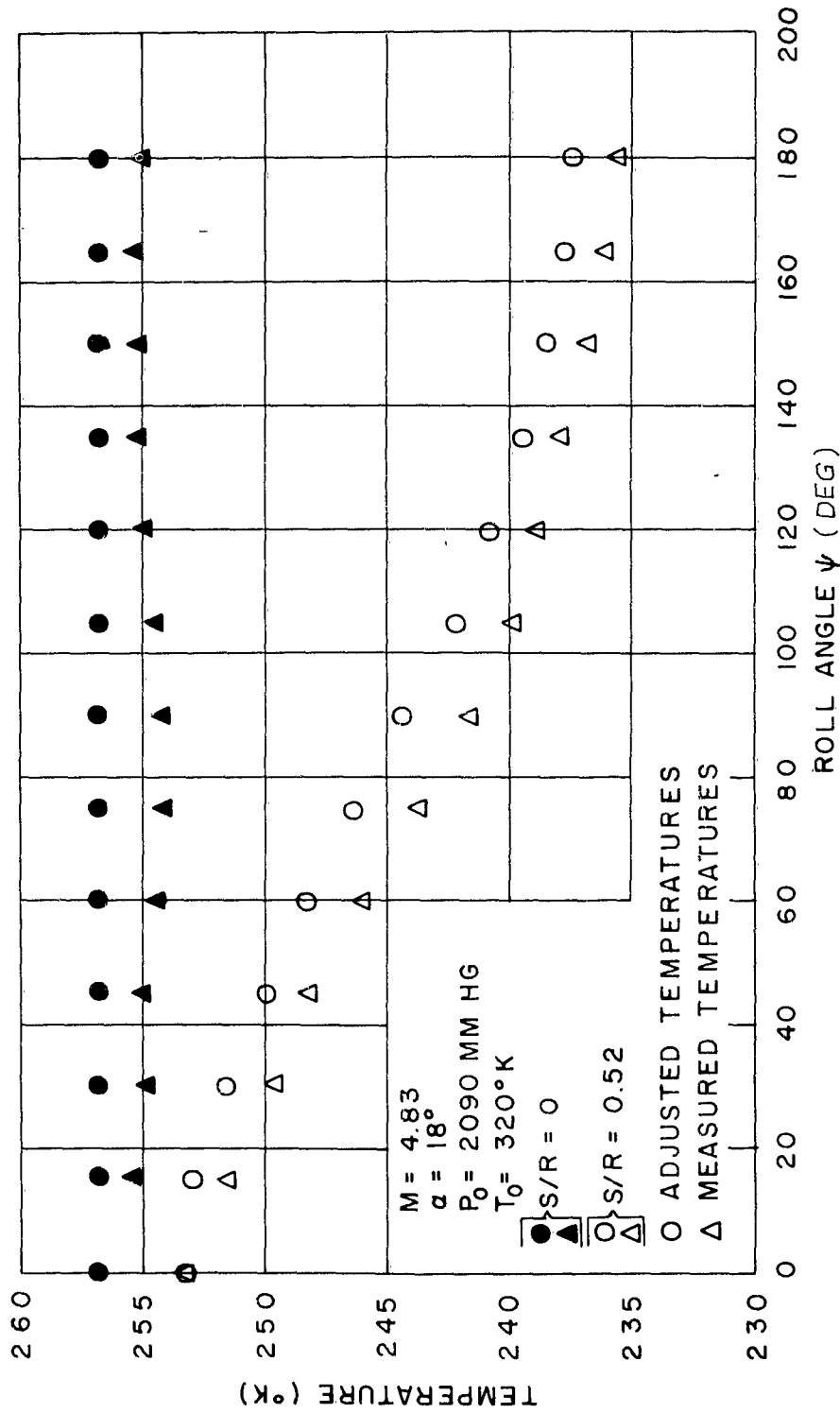


FIG. 13 COMPARISON BETWEEN ADJUSTED AND MEASURED TEMPERATURES ON THE SURFACE OF THE SPHERE - CONE MODEL AT  $M = 4.83$ ,  $\alpha = 18^{\circ}$ , AND  $S/R = 0$ , AND  $0.52$

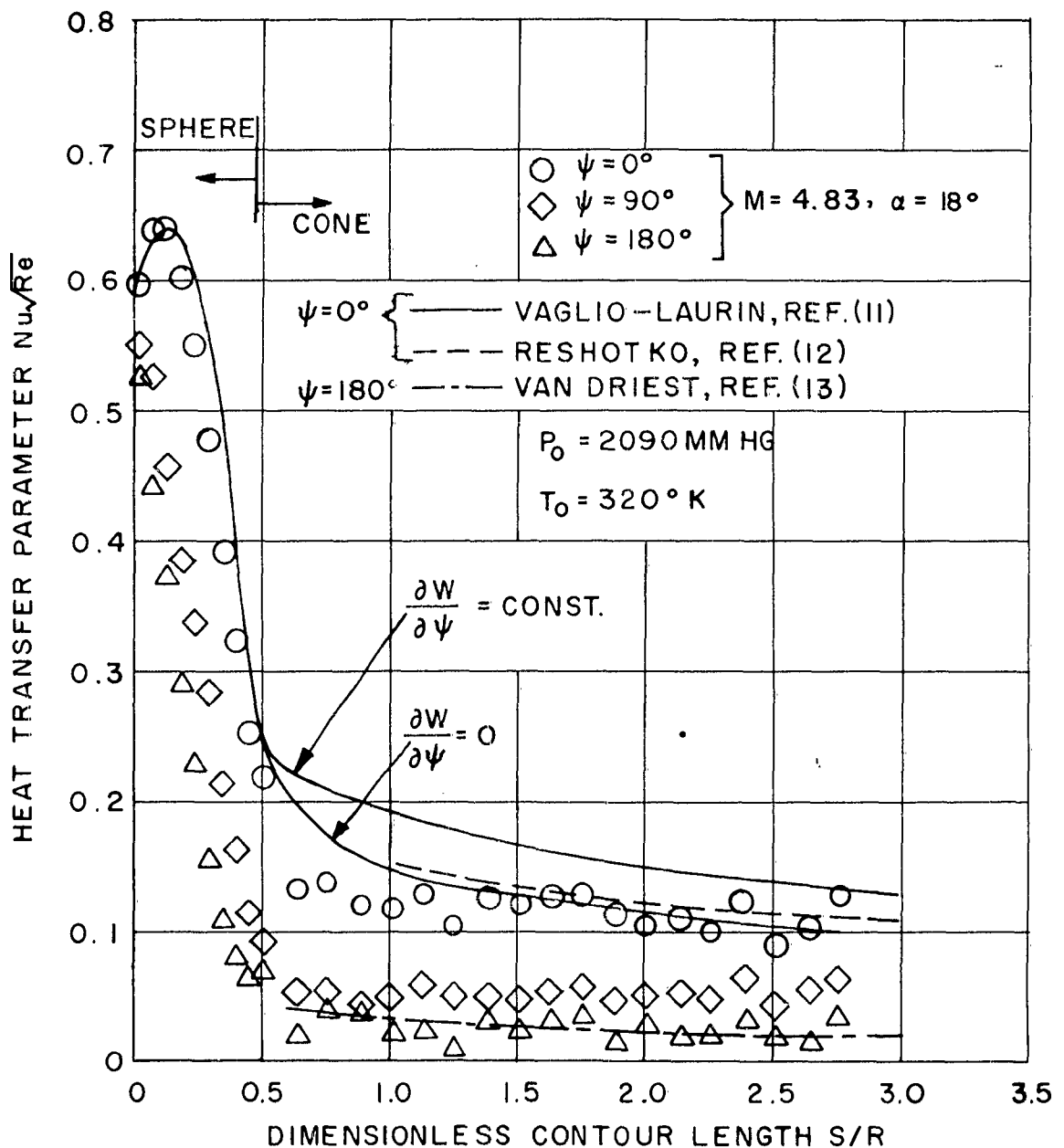


FIG.14 HEAT-TRANSFER DISTRIBUTION TO THE SURFACE OF A SPHERE - CONE MODEL AT  $M=4.83$  AND  $\alpha=18^\circ$

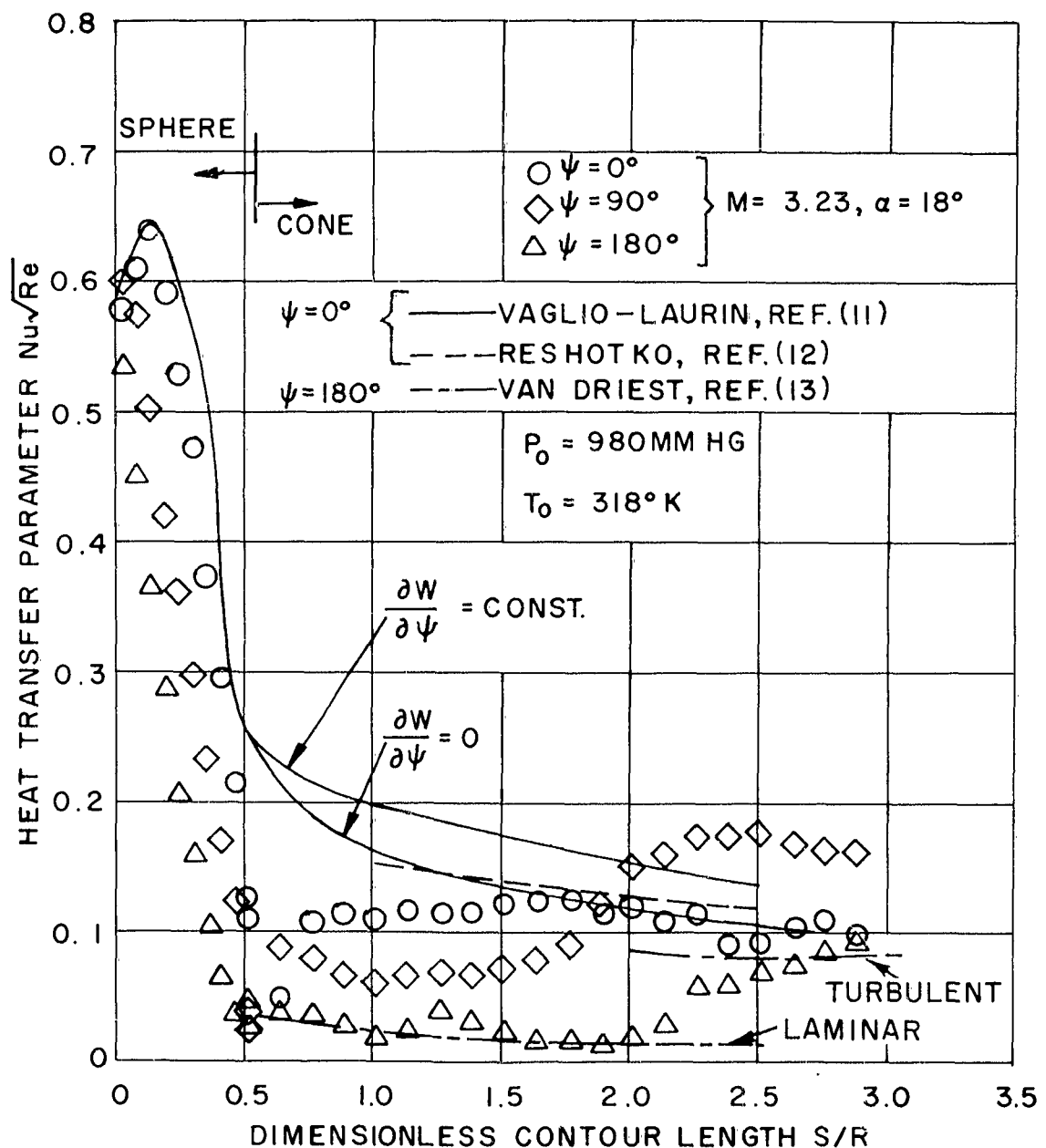


FIG.15 HEAT-TRANSFER DISTRIBUTION TO THE SURFACE OF A SPHERE - CONE MODEL AT  $M = 3.23$  AND  $\alpha = 18^\circ$

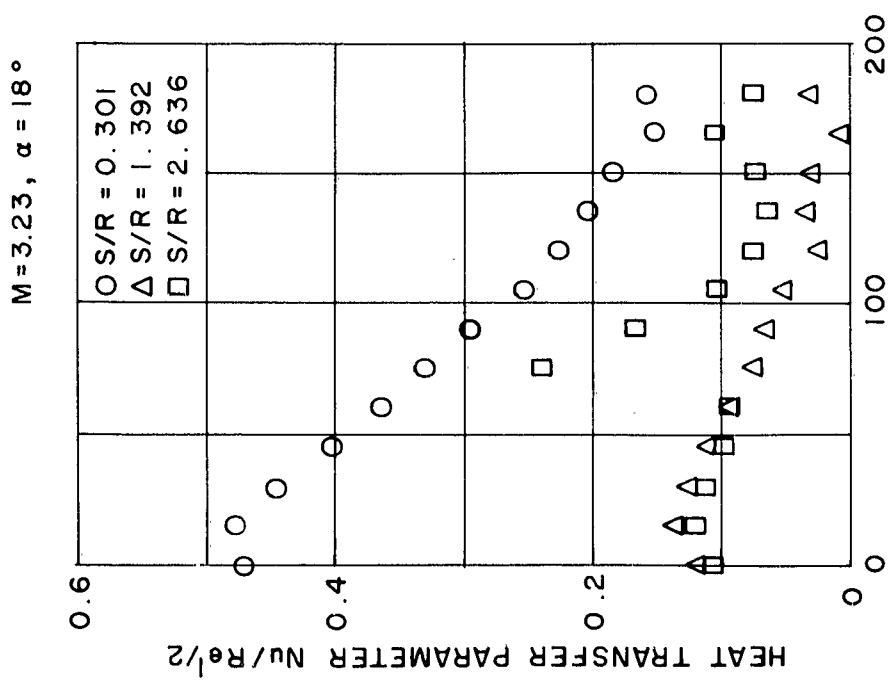


FIG. 16 HEAT TRANSFER VERSUS ROLL ANGLE FOR CONSTANT VALUES OF  $S/R = 0.301, 1.392$  AND  $2.636$  AT  $M = 3.23$  AND  $\alpha = 18^\circ$

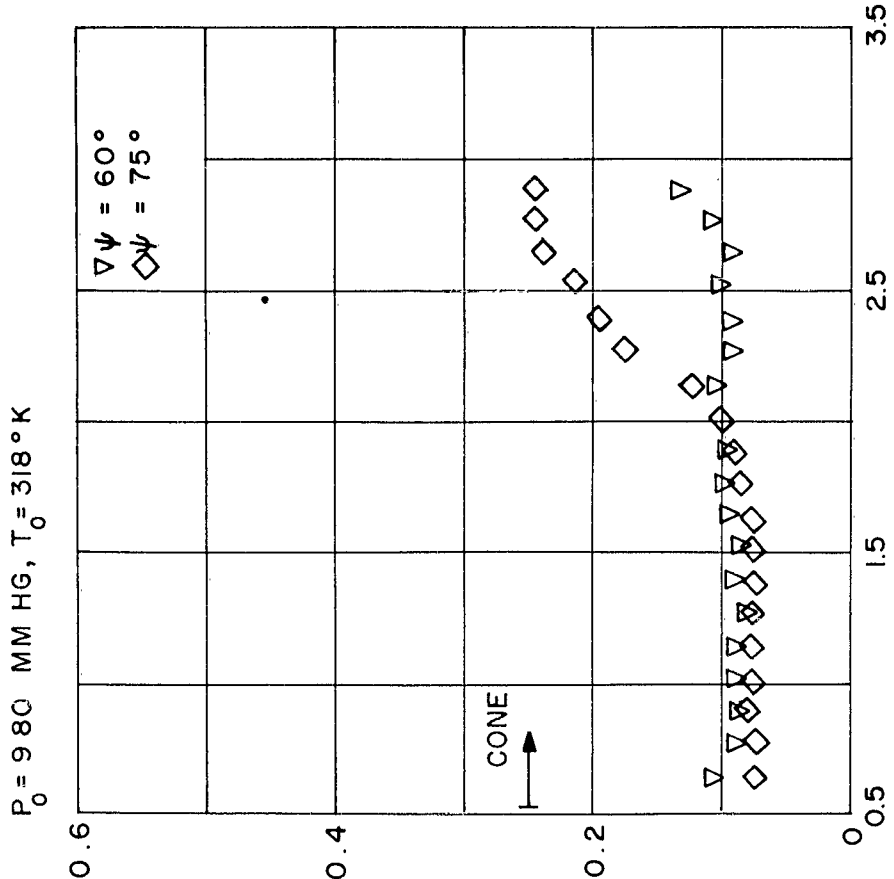


FIG. 17 HEAT TRANSFER VERSUS  $S/R$  FOR CONSTANT VALUES OF  $\psi = 60^\circ$  AND  $75^\circ$  AT  $M = 3.23$  AND  $\alpha = 18^\circ$

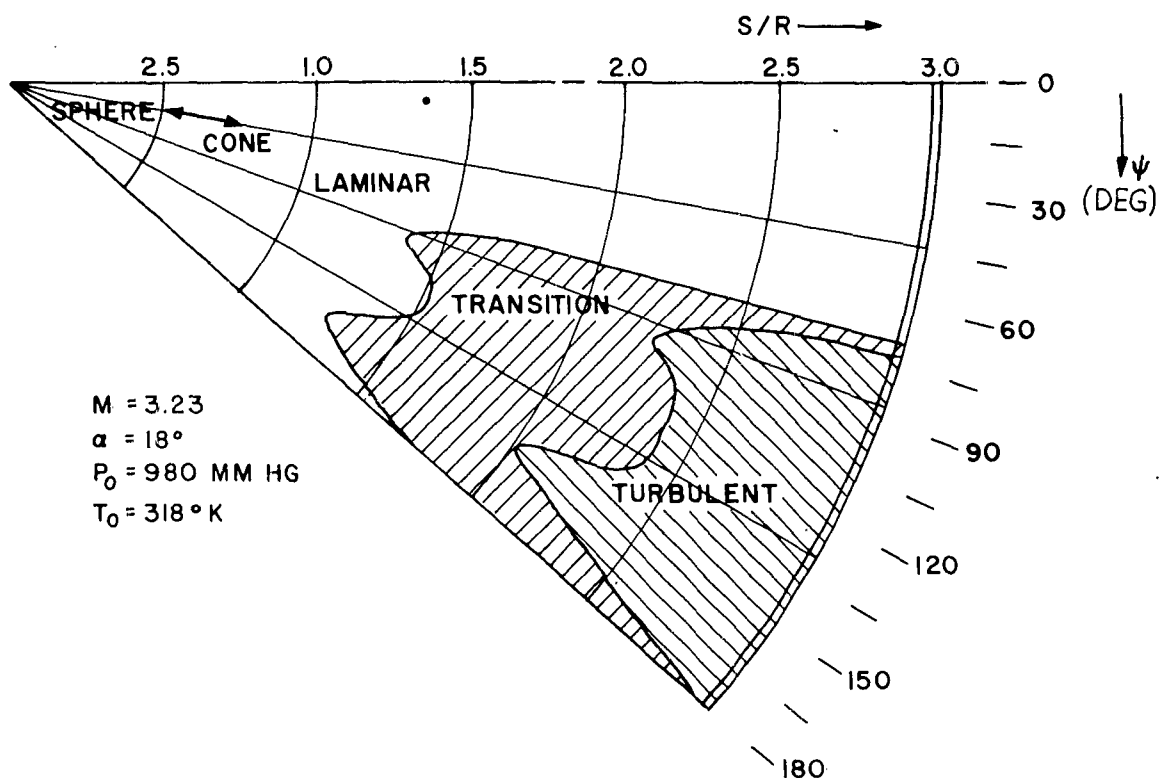


FIG.18 THE REGIONS OF LAMINAR, TRANSITIONAL AND TURBULENT BOUNDARY LAYERS AT  $M = 3.23$ ,  $\alpha = 18^\circ$

NOLTR 62-35

Table 1  
THERMOJUNCTION AND PRESSURE ORIFICE LOCATIONS

THERMOJUNCTION LOCATIONS			PRESSURE ORIFICE LOCATIONS						
SPHERE	CONE		SPHERE			CONE			
	Station	S/R	Station	S/R	Station	S/R	Station	S/R	Station
1	0.	10	0.645	20	1.890	A	0.068	F	0.769
2	0.068	11	0.769	21	2.014	B	0.136	G	1.112
3	0.136	12	0.894	22	2.138	C	0.258	H	1.454
4	0.204	13	1.018	23	2.263	D	0.407	I	1.796
5	0.305	14	1.143	24	2.387	E	0.520	J	2.138
6	0.356	15	1.267	25	2.512			K	2.481
7	0.407	16	1.392	26	2.636				
8	0.455	17	1.516	27	2.761				
9	0.520	18	1.640	28	2.885				
		19	1.765	29	3.010				

Table 2  
 PRESSURE DISTRIBUTION ON SPHERE-CONE MODEL  
 MACH NUMBER = 4.8  
 ANGLE OF ATTACK = 18.0 DEGREES  
 SUPPLY PRESSURE = 2090.0 MILLIMETERS OF HG.  
 SUPPLY TEMPERATURE = 320.0 DEGREES KELVIN

ROLL ANGLE	DIMENSIONLESS CONTOUR LENGTH / (PITOT PRESSURE) / (LOCAL STATIC PRESSURE)							
	0.407	0.520	0.769	1.112	1.454	1.796	2.138	2.481
0	0.9909	0.9949	0.8642	0.5128	0.2849	0.2658	0.2764	0.2983
5	0.9905	0.9934	0.8612	0.5101	0.2834	0.2639	0.2736	0.2878
10	0.9887	0.9888	0.8566	0.5052	0.2802	0.2602	0.2707	0.2839
15	0.9865	0.9851	0.8476	0.4980	0.2749	0.2558	0.2646	0.2765
20	0.9812	0.9778	0.8351	0.4862	0.2675	0.2487	0.2561	0.2661
25	0.9777	0.9697	0.8201	0.4735	0.2594	0.2416	0.2568	0.2746
30	0.9724	0.9607	0.8052	0.4596	0.2504	0.2313	0.2558	0.2704
35	0.9656	0.9487	0.7859	0.4437	0.2384	0.2216	0.2240	0.2314
40	0.9595	0.9350	0.7650	0.4239	0.2274	0.2076	0.2086	0.2143
45	0.9531	0.9198	0.7431	0.4012	0.2096	0.1960	0.1930	0.1971
50	0.9465	0.9049	0.7217	0.3865	0.2013	0.1894	0.1801	0.1852
55	0.9382	0.8906	0.6985	0.3675	0.1896	0.1761	0.1681	0.1706
60	0.9282	0.8724	0.6724	0.3471	0.1759	0.1644	0.1541	0.1547
65	0.9193	0.8566	0.6487	0.3266	0.1642	0.1519	0.1429	0.1409
70	0.9094	0.8390	0.6230	0.3069	0.1525	0.1405	0.1321	0.1280
75	0.9003	0.8222	0.5995	0.2881	0.1412	0.1300	0.1205	0.1153
80	0.8893	0.8038	0.5742	0.2699	0.1299	0.1202	0.1100	0.1051
85	0.8803	0.7860	0.5480	0.2504	0.1187	0.1116	0.1017	0.0940
90	0.8705	0.7652	0.5216	0.2331	0.1058	0.1031	0.0907	0.0809
95	0.8617	0.7489	0.5004	0.2131	0.1133	0.0994	0.0786	0.0691
100	0.8526	0.7339	0.4808	0.2043	0.1062	0.0941	0.0731	0.0648
105	0.8436	0.7181	0.4622	0.1910	0.0997	0.0877	0.0684	0.0594
110	0.8360	0.7027	0.4454	0.1788	0.0931	0.0816	0.0640	0.0557
115	0.8272	0.6877	0.4263	0.1668	0.0867	0.0762	0.0601	0.0510
120	0.8184	0.6729	0.4092	0.1563	0.0640	0.0711	0.0564	0.0472
125	0.8111	0.6599	0.3923	0.1466	0.0589	0.0674	0.0525	0.0433
130	0.8045	0.6484	0.3780	0.1378	0.0549	0.0638	0.0489	0.0403
135	0.7982	0.6369	0.3648	0.1295	0.0506	0.0604	0.0449	0.0362
140	0.7943	0.6294	0.3565	0.1229	0.0464	0.0581	0.0411	0.0322
145	0.7892	0.6216	0.3471	0.1178	0.0444	0.0564	0.0393	0.0322
150	0.7855	0.6145	0.3399	0.1133	0.0422	0.0545	0.0388	0.0320
155	0.7818	0.6098	0.3320	0.1092	0.0408	0.0542	0.0386	0.0325
160	0.7791	0.6045	0.3266	0.1063	0.0391	0.0525	0.0394	0.0330
165	0.7765	0.6003	0.3227	0.1033	0.0376	0.0521	0.0383	0.0337
170	0.7755	0.5979	0.3201	0.1014	0.0359	0.0515	0.0381	0.0257
175	0.7743	0.5969	0.3178	0.1001	0.0347	0.0501	0.0381	0.0257
180	0.7742	0.5966	0.3176	0.0995	0.0256	0.0470	0.0261	0.0255

**Table 2 (cont'd.)**  
 PRESSURE DISTRIBUTION ON SPHERE-CONE MODEL

MACH NUMBER = 3.2  
 ANGLE OF ATTACK = 18.0 DEGREES  
 SUPPLY PRESSURE = 980.0 MILLIPETERS OF HG.  
 SUPPLY TEMPERATURE = 319.0 DEGREES KELVIN

RELL ANGLE	DIMENSIONLESS CONTOUR LENGTH							
	0.407	0.520	0.769	1.112	1.454	1.796	2.138	2.481
0	0.9682	0.9956	0.8663	0.5366	0.3154	0.3282	0.3386	0.3545
5	0.9664	0.9956	0.8643	0.5355	0.3158	0.3260	0.3337	0.3523
10	0.9651	0.9943	0.8557	0.5304	0.3125	0.3229	0.3293	0.3434
15	0.9624	0.9870	0.8469	0.5204	0.3070	0.3180	0.3224	0.3403
20	0.9589	0.9777	0.8351	0.5094	0.3006	0.3103	0.3143	0.3255
25	0.9554	0.9671	0.8201	0.4964	0.2930	0.2983	0.3034	0.3165
30	0.9523	0.9585	0.8031	0.4840	0.2855	0.2908	0.3001	0.2997
35	0.9485	0.9487	0.7861	0.4720	0.2767	0.2751	0.2791	0.2866
40	0.9401	0.9341	0.7638	0.4506	0.2619	0.2572	0.2581	0.2694
45	0.9339	0.9209	0.7450	0.4334	0.2504	0.2422	0.2469	0.2526
50	0.9280	0.9081	0.7249	0.4124	0.2360	0.2285	0.2303	0.2356
55	0.9187	0.8915	0.6999	0.3907	0.2203	0.2139	0.2152	0.2203
60	0.9094	0.8738	0.6754	0.3704	0.2053	0.1971	0.2000	0.2044
65	0.8992	0.8575	0.6513	0.3529	0.1947	0.1836	0.1861	0.1890
70	0.8726	0.8418	0.6301	0.3337	0.1799	0.1708	0.1726	0.1759
75	0.8846	0.8267	0.6091	0.3167	0.1682	0.1554	0.1613	0.1593
80	0.8747	0.8113	0.5887	0.2994	0.1567	0.1439	0.1485	0.1461
85	0.8641	0.7943	0.5669	0.2802	0.1445	0.1308	0.1370	0.1317
90	0.8537	0.7739	0.5425	0.2590	0.1302	0.1162	0.1260	0.1162
95	0.8449	0.7585	0.5255	0.2482	0.1213	0.1074	0.1138	0.1039
100	0.8336	0.7417	0.5039	0.2334	0.1151	0.1001	0.1034	0.0944
105	0.8274	0.7257	0.4835	0.2186	0.1063	0.0916	0.0957	0.0869
110	0.8177	0.7103	0.4650	0.2069	0.0972	0.0835	0.0895	0.0796
115	0.8080	0.6959	0.4464	0.1936	0.0906	0.0769	0.0840	0.0738
120	0.8007	0.6820	0.4303	0.1817	0.0846	0.0707	0.0785	0.0694
125	0.7918	0.6674	0.4139	0.1722	0.0802	0.0650	0.0738	0.0636
130	0.7819	0.6548	0.3976	0.1618	0.0731	0.0623	0.0654	0.0588
135	0.7757	0.6433	0.3848	0.1538	0.0698	0.0579	0.0608	0.0548
140	0.7693	0.6325	0.3706	0.1463	0.0659	0.0570	0.0614	0.0566
145	0.7615	0.6239	0.3596	0.1401	0.0619	0.0555	0.0577	0.0559
150	0.7567	0.6150	0.3514	0.1357	0.0568	0.0559	0.0577	0.0559
155	0.7545	0.6095	0.3454	0.1315	0.0568	0.0579	0.0586	0.0572
160	0.7503	0.6038	0.3399	0.1260	0.0552	0.0577	0.0586	0.0586
165	0.7470	0.5989	0.3348	0.1224	0.0522	0.0583	0.0592	0.0601
170	0.7461	0.5937	0.3313	0.1218	0.0524	0.0586	0.0594	0.0625
175	0.7461	0.5940	0.3293	0.1207	0.0522	0.0586	0.0606	0.0625
180	0.7461	0.5940	0.3293	0.1176	0.0510	0.0575	0.0588	0.0639

**Table 2 (cont'd.)**  
 PRESSURE DISTRIBUTION ON SPHERE-CCNE MODEL

MACH NUMBER = 5.2  
 ANGLE OF ATTACK = 4.0 DEGREES  
 SUPPLY PRESSURE = 980.0 MILLIMETERS OF HG.  
 SUPPLY TEMPERATURE = 318.0 DEGREES KELVIN

ROLL ANGLE	DIMENSIONLESS CONTOUR LENGTH							
	0.407	0.520	0.769	1.112	1.454	1.796	2.138	2.481
0	0.9624	0.7110	0.7165	0.3593	0.1817	0.1843	0.1757	0.1741
5	0.9609	0.7177	0.7143	0.3587	0.1812	0.1834	0.1753	0.1737
10	0.9596	0.7224	0.7094	0.3571	0.1906	0.1817	0.1735	0.1728
15	0.9569	0.9173	0.7054	0.3549	0.1799	0.1606	0.1722	0.1713
20	0.9540	0.9114	0.6992	0.3516	0.1774	0.1777	0.1706	0.1695
25	0.9505	0.9063	0.6928	0.3474	0.1738	0.1783	0.1680	0.1666
30	0.9481	0.9033	0.6855	0.3446	0.1772	0.1761	0.1638	0.1640
35	0.9454	0.6946	0.6787	0.3423	0.1757	0.1741	0.1618	0.1604
40	0.9425	0.6860	0.6692	0.3372	0.1737	0.1710	0.1591	0.1571
45	0.9401	0.5773	0.6581	0.3312	0.1719	0.1673	0.1562	0.1543
50	0.9388	0.8720	0.6495	0.3253	0.1668	0.1631	0.1529	0.1525
55	0.9388	0.8650	0.6378	0.3171	0.1629	0.1580	0.1485	0.1498
60	0.9383	0.8601	0.6278	0.3112	0.1591	0.1536	0.1450	0.1459
65	0.9392	0.8557	0.6188	0.3059	0.1551	0.1509	0.1421	0.1421
70	0.9392	0.8517	0.6082	0.2966	0.1512	0.1474	0.1379	0.1288
75	0.9410	0.8539	0.6027	0.2895	0.1481	0.1450	0.1361	0.1350
80	0.9397	0.8524	0.5962	0.2818	0.1454	0.1410	0.1344	0.1324
85	0.9372	0.8480	0.5903	0.2747	0.1414	0.1377	0.1313	0.1221
90	0.9350	0.8429	0.5834	0.2694	0.1368	0.1344	0.1288	0.1262
95	0.9348	0.3393	0.5783	0.2639	0.1326	0.1221	0.1264	0.1220
100	0.9341	0.8363	0.5724	0.2590	0.1291	0.1262	0.1231	0.1189
105	0.9326	0.8340	0.5662	0.2530	0.1251	0.1231	0.1193	0.1145
110	0.9322	0.8318	0.5587	0.2471	0.1218	0.1207	0.1158	0.1129
115	0.9306	0.8294	0.5518	0.2422	0.1171	0.1173	0.1120	0.1114
120	0.9291	0.8256	0.5441	0.2373	0.1138	0.1154	0.1109	0.1101
125	0.9286	0.8219	0.5383	0.2336	0.1143	0.1123	0.1083	0.1059
130	0.9273	0.8161	0.5324	0.2285	0.1120	0.1090	0.1070	0.1036
135	0.9255	0.6128	0.5266	0.2241	0.1092	0.1059	0.1017	0.1008
140	0.7262	0.6113	0.5242	0.2262	0.1094	0.1056	0.1012	0.1014
145	0.7246	0.8080	0.5204	0.2270	0.1076	0.1054	0.0992	0.1008
150	0.9231	0.8060	0.5176	0.2254	0.1065	0.1039	0.0970	0.1039
155	0.7218	0.8038	0.5151	0.2243	0.1043	0.1023	0.0952	0.1030
160	0.9196	0.3015	0.5138	0.2217	0.1021	0.1008	0.0955	0.1008
165	0.9198	0.7993	0.5131	0.2163	0.1003	0.0997	0.0957	0.1003
170	0.9187	0.7993	0.5120	0.2172	0.0986	0.0979	0.0957	0.0994
175	0.7187	0.7993	0.5109	0.2164	0.0963	0.0972	0.0948	0.0992
180	0.9187	0.7993	0.5109	0.2159	0.0972	0.0944	0.0957	0.0988

**Table 2 (cont'd.)**  
 PRESSURE DISTRIBUTION ON SPHERE-CONE MODEL

MACH NUMBER = 4.8  
 ANGLE OF ATTACK = 6.0 DEGREES  
 SUPPLY PRESSURE = 2090.0 MILLIMETERS OF HG.  
 SUPPLY TEMPERATURE = 320.0 DEGREES KELVIN

ROLL ANGLE	DIMENSIONLESS CONTOUR LENGTH						
	0.407	0.520	0.767	1.112	1.454	1.796	2.138
0.0668	0.136	0.258	0.407	0.520	0.767	1.112	1.454
							(LOCAL STATIC PRESSURE)/(TOTAL PRESSURE)
0	0.9753	0.9191	0.6785	0.3292	0.1693	0.1429	0.1360
5	0.9740	0.9184	0.6772	0.3267	0.1666	0.1422	0.1378
10	0.9740	0.9171	0.6755	0.3266	0.1649	0.1421	0.1378
15	0.9725	0.9152	0.6728	0.3233	0.1637	0.1405	0.1372
20	0.9691	0.9123	0.6681	0.3187	0.1615	0.1377	0.1348
25	0.9664	0.9076	0.6613	0.3145	0.1584	0.1350	0.1329
30	0.9642	0.9044	0.6564	0.3105	0.1573	0.1319	0.1312
35	0.9625	0.9014	0.6493	0.5064	0.1541	0.1296	0.1291
40	0.9605	0.9003	0.6421	0.5007	0.1503	0.1262	0.1252
45	0.9586	0.8958	0.6363	0.2965	0.1473	0.1233	0.1235
50	0.9551	0.8902	0.6297	0.2921	0.1449	0.1206	0.1203
55	0.9515	0.8856	0.6181	0.2833	0.1383	0.1162	0.1157
60	0.9488	0.6792	0.6150	0.2797	0.1329	0.1149	0.1144
65	0.9448	0.8721	0.6024	0.2725	0.1297	0.1101	0.1106
70	0.9404	0.8650	0.5929	0.2662	0.1257	0.1064	0.1081
75	0.9404	0.8618	0.5856	0.2611	0.1245	0.1049	0.1034
80	0.9367	0.8559	0.5794	0.2574	0.1211	0.1029	0.1008
85	0.9321	0.8486	0.5669	0.2483	0.1181	0.0990	0.0978
90	0.9285	0.8421	0.5530	0.2400	0.1105	0.0959	0.0953
95	0.9252	0.8346	0.5488	0.2323	0.1069	0.0934	0.0903
100	0.9221	0.8301	0.5419	0.2280	0.1042	0.0910	0.0890
105	0.9186	0.8247	0.5345	0.2245	0.1022	0.0883	0.0865
110	0.9157	0.8174	0.5275	0.2186	0.0992	0.0846	0.0836
115	0.9120	0.8110	0.5204	0.2137	0.0971	0.0821	0.0824
120	0.9091	0.8057	0.5137	0.2093	0.0949	0.0802	0.0796
125	0.9076	0.7995	0.5073	0.2052	0.0917	0.0775	0.0769
130	0.9052	0.7948	0.5002	0.2007	0.0897	0.0757	0.0748
135	0.9020	0.7872	0.4948	0.1963	0.0863	0.0730	0.0745
140	0.8998	0.7834	0.4919	0.1965	0.0885	0.0743	0.0735
145	0.8990	0.7802	0.4889	0.1952	0.0865	0.0738	0.0711
150	0.8980	0.7770	0.4853	0.1902	0.0843	0.0725	0.0704
155	0.8963	0.7760	0.4841	0.1835	0.0831	0.0709	0.0699
160	0.8953	0.7743	0.4814	0.1873	0.0823	0.0699	0.0684
165	0.8963	0.7731	0.4804	0.1865	0.0807	0.0696	0.0681
170	0.8963	0.7726	0.4789	0.1853	0.0807	0.0696	0.0684
175	0.8963	0.7726	0.4789	0.1845	0.0802	0.0693	0.0679
180	0.8963	0.7726	0.4784	0.1838	0.0791	0.0682	0.0676

**Table 3**  
 TEMPERATURE DISTRIBUTION ON SPHERE-CONE MODEL. (NOSE SECTION)

MACH NUMBER = 4.82  
 ANGLE OF ATTACK = 18 DEGREES  
 SUPPLY PRESSURE = 2090 MILLIMETERS OF HG.  
 SUPPLY TEMPERATURE = 320.0 DEGREES KELVIN

S/R	D	ROLL ANGLE (DEGREES)								165	180
		0	15	30	45	60	75	90	105		
0.	0.	256.8	255.4	254.8	255.0	254.4	254.1	254.0	254.5	255.2	255.3
0.	0.500	242.0	240.4	240.3	239.9	239.8	239.3	239.2	240.0	240.7	240.2
0.	0.68	258.6	257.0	255.9	255.8	254.8	254.2	253.6	253.4	253.0	252.6
0.	0.136	259.7	257.9	256.9	256.6	256.1	254.7	253.6	252.5	251.3	250.9
0.	0.136	246.8	243.9	242.9	242.2	241.0	240.4	239.9	239.7	239.2	238.6
0.	0.204	259.7	258.0	256.3	255.7	253.8	252.6	250.9	250.0	249.2	247.6
0.	0.305	258.8	256.9	255.3	254.2	252.1	249.9	248.0	246.5	245.4	242.7
0.	0.305	0.500	250.9	248.7	247.4	246.6	244.9	243.2	241.9	240.1	237.9
0.	0.305	0.375	253.8	251.8	250.4	249.6	247.7	245.3	244.3	242.1	239.2
0.	0.305	0.250	256.5	254.5	253.1	252.1	250.2	248.1	246.3	243.8	240.5
0.	0.305	0.125	256.5	254.5	253.1	252.1	250.4	248.5	246.4	244.8	241.8
0.	0.356	0.	257.6	255.8	254.1	252.8	251.7	249.1	247.0	245.5	240.7
0.	0.407	0.	256.1	254.5	252.7	251.3	249.1	247.0	244.3	243.1	239.7
0.	0.407	0.300	246.5	246.5	246.5	245.9	243.9	242.1	240.7	237.9	235.6
0.	0.455	0.	255.1	253.3	251.4	250.0	247.5	245.5	243.3	242.0	239.8
0.	0.520	0.	253.3	251.6	249.5	248.2	245.9	243.7	241.7	239.9	236.8
0.	0.520	0.500	248.5	246.5	244.5	243.5	241.9	240.0	238.5	236.3	234.5
0.	0.520	0.375	249.7	248.1	246.3	245.3	243.2	241.3	239.6	237.2	235.2
0.	0.520	0.250	251.0	249.4	247.5	246.4	244.3	242.3	240.5	238.8	235.9
0.	0.520	0.125	252.1	250.4	248.6	247.3	245.0	243.0	241.1	239.4	236.6

Table 3 (cont'd.)

MACH NUMBER = 4.62  
 ANGLE OF ATTACK = 18 DEGREES  
 SUPPLY PRESSURE = 2090 MILLIBARERS OF HG.  
 SUPPLY TEMPERATURE = 320.0 DEGREES KELVIN

S/R	D	ROLL ANGLE (DEGREES)							135	150	165	180	
		0	15	30	45	60	75	90					
0.645	0°	251.7	248.3	246.7	244.8	243.6	241.3	239.7	237.9	236.8	235.0	234.5	233.9
0.645	0.500	251.0	251.2	249.8	247.6	246.0	243.4	241.1	237.7	236.1	235.1	234.3	233.0
0.769	0°	249.8	248.1	246.6	244.5	243.1	240.8	238.6	236.8	235.6	234.7	233.9	233.4
0.769	0.500	248.1	246.6	245.6	244.5	243.1	240.8	238.8	236.0	235.0	234.0	233.1	232.6
0.894	0°	251.0	249.6	247.2	245.3	242.7	240.2	237.6	235.1	234.5	233.7	232.9	231.8
0.894	0.500	248.2	246.8	244.4	242.8	240.3	238.1	235.8	234.0	233.4	232.5	231.4	231.1
1.018	0°	251.1	249.7	247.1	245.1	242.2	239.4	236.7	234.6	233.4	232.1	231.4	230.5
1.018	0.500	248.4	246.9	244.3	242.4	240.3	238.8	236.0	234.1	232.9	231.7	230.0	229.5
1.143	0°	251.4	250.1	247.3	245.3	242.0	238.9	236.2	234.9	233.6	232.6	231.5	229.8
1.143	0.500	248.6	247.0	244.2	242.0	240.0	239.3	236.6	234.3	232.3	231.0	230.6	230.1
1.267	0°	251.5	250.2	247.2	245.2	242.3	241.3	238.2	235.1	233.0	232.4	231.4	230.8
1.267	0.500	249.1	247.5	244.4	242.0	240.0	239.0	236.3	234.6	233.4	232.1	231.4	230.2
1.392	0°	252.2	250.9	247.6	245.1	242.4	241.4	238.2	235.0	233.1	232.0	231.9	230.0
1.392	0.500	249.6	248.0	244.7	242.7	240.1	238.5	236.0	234.3	232.6	231.1	230.5	229.5
1.516	0°	252.6	251.3	247.6	245.6	242.9	241.2	237.9	234.6	232.3	231.0	229.7	228.5
1.516	0.500	250.0	248.3	244.8	242.1	240.1	238.7	235.7	233.6	231.8	230.4	229.5	228.8
1.640	0°	253.1	251.6	248.2	245.1	242.3	241.3	237.3	234.5	232.8	231.4	229.8	228.5
1.640	0.500	250.4	248.7	245.2	242.2	240.7	238.7	235.6	233.7	231.3	230.1	228.8	227.0
1.765	0°	253.6	252.1	248.5	245.5	242.5	241.3	237.7	234.6	232.3	231.0	229.7	228.1
1.765	0.500	252.6	250.6	247.6	244.9	242.6	241.2	237.9	234.6	232.3	231.0	229.7	228.0
1.890	0°	253.9	252.5	248.6	245.1	242.6	241.1	237.4	235.0	233.6	232.1	230.4	229.2
1.890	0.500	251.5	249.7	245.7	242.4	240.6	238.6	235.3	233.5	232.0	230.8	229.8	228.0
2.014	0°	254.5	253.0	249.0	245.3	242.1	241.2	237.4	234.5	232.0	230.4	229.0	227.5
2.014	0.500	252.1	250.2	246.0	243.5	240.5	238.7	235.3	233.9	231.7	230.1	228.7	227.4
2.138	0°	255.4	253.8	249.3	245.4	242.4	241.2	237.3	234.6	232.3	231.0	229.4	228.3
2.138	0.500	253.0	251.1	246.4	242.7	240.7	238.9	235.3	233.7	231.3	230.0	228.8	227.7
2.263	0°	256.6	254.6	250.0	245.7	242.4	241.4	237.3	234.6	232.7	231.3	229.9	228.4
2.263	0.500	254.4	252.2	247.1	243.0	240.0	239.0	235.3	233.9	231.7	230.3	229.9	228.7
2.387	0°	258.6	256.4	251.2	246.3	241.7	241.7	237.6	234.0	232.4	230.1	228.4	227.6
2.387	0.500	256.4	253.6	248.3	243.4	240.1	239.1	235.3	232.1	229.3	227.1	225.9	224.7
2.512	0°	260.1	258.1	252.3	246.5	241.9	241.9	237.5	234.3	232.2	230.7	228.3	226.3
2.512	0.500	258.5	256.1	249.8	244.2	240.2	239.7	235.6	232.3	229.4	227.0	226.0	225.0
2.636	0°	262.0	260.1	254.0	247.8	242.2	242.2	237.8	234.0	232.9	231.7	229.5	228.6
2.636	0.500	260.5	258.4	251.6	245.2	240.8	239.8	235.7	232.3	229.5	227.3	226.1	225.2
2.761	0°	263.6	261.6	255.6	249.0	242.0	242.8	238.1	234.4	231.3	228.8	226.6	226.3
2.761	0.500	262.4	260.3	253.5	246.3	240.3	239.9	235.9	232.5	229.7	227.5	226.4	225.0
2.885	0°	263.0	261.2	255.6	249.1	242.4	242.4	237.7	234.0	232.3	231.0	228.7	226.8
2.885	0.500	262.8	261.0	255.1	247.7	240.8	236.3	235.7	232.9	230.1	228.1	226.4	225.9
3.010	0°	263.3	261.7	256.5	250.5	245.0	243.7	236.8	235.2	232.4	230.1	229.4	228.2
3.010	0.375	262.0	260.4	255.1	249.4	241.9	241.9	237.2	233.8	231.3	229.2	227.7	227.2
3.010	0.250	262.3	260.7	255.3	249.6	242.3	242.3	237.5	234.1	231.4	229.2	227.8	227.3
3.010	0.125	262.7	261.1	255.9	250.1	243.0	243.0	238.1	234.6	231.8	229.5	227.9	227.5

**Table 3 (cont'd.)**  
**TEMPERATURE DISTRIBUTION ON SPHERE-CONE MODEL. (NOSE SECTION)**

S/R	D	ROLL ANGLE (DEGREES)										165	180			
		0	15	30	45	60	75	90	105	120	135					
TEMPERATURE, °K																
MACH NUMBER = 3.23 ANGLE OF ATTACK = 18 DEGREES SUPPLY PRESSURE = 980 MILLIMETERS OF HG. SUPPLY TEMPERATURE = 318.0 DEGREES KELVIN																
0.	0.	266.6	265.8	265.7	264.9	264.5	264.0	263.7	264.4	264.3	264.4	264.5	264.6	264.5		
0.	0.500	246.0	246.0	248.0	245.5	245.1	245.5	244.5	244.7	244.7	245.7	245.6	244.8	244.2		
0.	0.668	268.4	267.6	267.7	266.3	265.3	264.4	263.5	263.5	262.9	262.4	262.1	261.9	261.8		
0.	136	0.	269.8	268.9	268.5	266.7	265.3	263.7	262.3	261.5	260.9	260.1	259.4	258.7		
0.	136	0.500	254.9	254.4	252.7	251.6	250.3	249.1	247.9	248.0	247.6	247.3	246.6	246.0		
0.	204	0.	269.5	268.8	268.0	266.3	264.4	262.6	260.7	259.8	258.5	257.3	256.4	255.5		
0.	305	0.	268.6	267.9	266.6	264.3	262.1	260.0	257.7	256.4	254.6	253.2	252.0	251.1		
0.	305	0.500	0.375	0.375	0.375	0.375	0.375	0.375	0.375	0.375	0.375	0.375	0.375	0.375		
0.	305	0.250	263.2	262.6	261.4	259.4	257.3	255.6	253.5	252.5	251.1	250.0	248.9	247.8		
0.	305	0.125	266.3	265.5	264.4	262.2	260.1	258.2	256.0	254.8	253.2	251.9	250.6	249.3		
0.	356	0.	267.3	266.7	265.5	263.1	260.6	258.5	256.0	254.4	252.6	251.0	249.1	248.8		
0.	407	0.	265.8	265.2	264.1	261.6	259.1	256.8	254.3	252.7	250.7	249.2	248.0	247.2		
0.	407	0.500	257.2	256.6	255.5	253.3	251.4	249.6	247.6	246.5	245.4	244.4	243.5	242.5		
0.	455	0.	264.6	264.0	262.8	260.2	257.7	255.3	252.9	251.1	249.1	247.7	246.8	246.0		
0.	520	0.	262.7	262.1	261.0	258.5	256.0	253.5	251.0	249.2	247.3	245.8	244.8	243.8		
0.	520	0.500	257.3	256.5	255.7	253.4	251.3	249.3	247.2	245.8	243.5	242.5	241.8	241.5		
0.	520	0.375	258.8	258.1	257.3	255.1	252.9	250.8	248.6	247.1	245.7	244.5	243.4	242.3		
0.	520	0.250	260.4	259.7	258.8	256.6	254.3	252.0	249.7	248.1	246.6	245.3	244.2	243.0		
0.	520	0.125	261.0	261.0	261.0	259.7	258.1	256.0	254.3	252.0	249.9	247.2	246.7	243.4		

Table 3 (cont'd.)

## TEMPERATURE DISTRIBUTION ON SPHERE-CONE MODEL, (CONE SECTION)

MACH NUMBER = 3.023  
 ANGLE OF ATTACK = 18 DEGREES  
 SUPPLY PRESSURE = 980 MILLIMETERS OF HG.  
 SUPPLY TEMPERATURE = 318.0 DEGREES KELVIN

S/R	D	ROLL ANGLE (DEGREES)								150	165	180
		0	15	30	45	60	75	90	105			
0.645 0.	261.3	260.8	259.7	257.2	254.6	252.0	249.4	247.4	245.4	244.1	243.0	242.4
0.645 0.500	257.4	256.7	255.8	253.6	251.3	249.1	246.9	245.3	243.8	242.7	241.7	240.9
0.769 0.	261.3	260.7	259.4	256.9	254.1	251.4	248.7	246.6	244.4	242.9	242.0	241.4
0.769 0.500	257.8	257.0	255.8	253.6	251.2	248.7	246.3	244.7	243.0	241.8	240.7	240.0
0.894 0.	261.5	260.8	259.4	256.6	253.6	250.7	248.0	245.7	243.3	241.8	240.8	240.3
0.894 0.500	258.5	257.5	256.0	253.5	250.8	248.2	245.7	243.9	242.1	240.8	239.7	238.9
1.018 0.	261.8	260.9	259.3	256.4	253.3	250.3	247.3	244.9	242.7	241.2	240.0	239.0
1.018 0.500	258.9	257.7	256.0	253.1	250.3	247.7	245.0	243.2	241.4	240.0	238.1	237.9
1.143 0.	262.3	261.2	259.5	256.3	253.1	250.1	246.9	244.4	242.3	240.8	239.5	238.4
1.143 0.500	259.3	257.8	255.8	252.7	249.7	247.1	244.7	242.4	240.7	239.3	238.1	237.1
1.267 0.	262.4	261.3	259.4	256.0	252.7	249.6	246.5	243.9	241.7	240.3	239.0	238.1
1.267 0.500	259.9	258.3	256.1	252.9	249.9	247.1	244.4	242.3	240.6	239.3	238.1	237.2
1.392 0.	263.1	261.9	259.8	256.3	253.0	249.8	246.8	244.3	242.3	240.9	239.6	238.5
1.392 0.500	260.4	258.7	256.5	253.1	250.0	247.2	244.5	242.5	240.4	239.5	238.3	237.0
1.516 0.	263.6	262.4	260.1	256.6	253.1	249.9	247.1	244.6	242.0	241.2	240.2	238.9
1.516 0.500	260.9	259.2	256.8	253.3	250.2	247.2	244.7	242.6	240.3	239.6	237.5	236.9
1.640 0.	264.1	262.9	260.5	257.1	253.7	250.4	248.1	245.5	243.5	242.0	241.5	239.8
1.640 0.500	261.4	260.4	259.8	257.3	253.9	250.7	247.7	245.6	243.4	242.5	240.4	239.4
1.765 0.	264.9	263.6	261.0	257.6	254.4	251.5	249.5	246.9	243.8	242.0	241.2	240.9
1.765 0.500	262.0	260.4	257.6	254.3	251.2	248.3	246.6	244.2	241.4	240.2	239.0	237.7
1.880 0.	265.5	264.2	261.6	258.1	255.0	252.5	251.2	248.0	246.7	243.9	243.5	242.1
1.880 0.500	262.9	261.3	258.4	255.0	252.0	249.6	246.1	244.3	242.3	241.0	240.2	238.4
2.014 0.	266.7	265.1	262.4	259.0	256.1	253.9	250.3	249.5	246.9	243.0	242.8	241.4
2.014 0.500	264.2	262.4	259.2	255.8	253.0	250.6	248.6	246.4	243.3	241.0	240.2	239.0
2.138 0.	268.1	266.3	263.3	259.7	256.8	255.6	254.7	250.7	246.8	243.9	243.5	242.8
2.138 0.500	265.9	263.7	260.5	256.7	253.7	252.2	250.9	247.5	244.3	243.5	242.6	240.8
2.263 0.	270.1	268.0	264.5	260.5	257.5	257.9	255.6	251.5	247.8	246.8	246.1	244.3
2.263 0.500	268.0	265.6	261.7	257.6	254.4	253.7	251.8	248.2	245.1	244.6	243.3	241.8
2.387 0.	272.4	270.2	266.3	261.7	258.5	259.9	256.6	252.6	248.7	247.5	246.9	245.7
2.387 0.500	270.6	268.0	263.5	258.8	255.2	255.2	252.5	249.1	245.7	245.0	244.1	243.7
2.512 0.	274.4	272.2	268.2	264.9	261.2	259.2	256.9	252.6	248.8	247.4	246.7	245.9
2.512 0.500	273.1	270.7	265.8	260.1	256.2	256.4	253.1	249.6	246.2	245.2	244.3	243.3
2.636 0.	276.5	274.4	270.2	264.5	260.8	262.1	257.6	253.2	249.2	247.5	246.9	246.5
2.636 0.500	275.3	273.1	268.4	261.7	257.5	257.4	253.6	249.9	246.5	245.0	244.1	243.8
2.761 0.	278.1	276.0	272.1	266.3	262.5	263.0	258.1	253.7	249.6	247.6	247.1	247.3
2.761 0.500	277.0	274.9	270.6	263.6	258.8	258.2	254.1	250.3	246.7	245.0	244.1	243.9
2.885 0.	288.5	285.0	278.9	277.1	273.7	268.7	265.2	258.9	254.5	250.4	248.0	247.8
2.885 0.500	277.5	274.9	271.1	267.4	262.3	260.4	255.7	251.9	248.2	246.1	245.5	246.0
3.010 0.	3010.0	0.375	277.9	276.1	272.7	267.4	262.3	260.4	256.7	252.7	248.9	246.7
3.010 0.250	278.2	276.3	272.8	267.6	263.0	261.6	256.7	253.0	249.7	247.9	246.9	247.5
3.010 0.125	278.6	276.8	273.5	268.2	264.1	263.0	257.9	253.7	249.7	247.4	246.9	247.9

Table 3 (cont'd.)  
TEMPERATURE DISTRIBUTION ON SPHERE-CONE NOSE. (NOSE SECTION)

S/R	D	0	15	30	45	60	75	90	105	120	135	150	165	180	ROLL ANGLE (DEGREES)	
															TEMPERATURE, °K	
0.	0.	265.3	265.1	264.3	263.5	263.1	263.2	262.6	262.6	262.9	263.2	263.1	263.3	262.2	262.2	262.2
0.	0.500	246.1	245.5	245.8	243.6	244.5	244.9	242.6	242.6	243.2	243.2	244.0	243.1	243.0	242.1	242.1
0.068	0.	266.1	265.7	264.7	263.5	262.6	262.4	261.7	261.6	262.0	262.3	262.0	262.4	262.4	262.4	262.4
0.136	0.	266.4	265.8	264.7	263.3	261.9	261.4	260.6	260.5	260.6	260.7	260.5	260.3	259.7	259.7	259.7
0.136	0.500	252.4	251.3	249.2	248.3	246.5	245.7	244.9	245.6	246.0	246.0	245.6	245.6	244.5	244.5	244.5
0.204	0.	265.7	265.1	263.7	262.5	260.4	259.8	258.9	258.8	258.8	258.8	258.8	258.6	257.5	257.5	257.5
0.305	0.	263.1	262.5	261.1	259.7	257.5	256.7	255.5	255.5	255.2	254.9	254.5	254.5	253.5	253.5	253.5
0.305	0.500	255.1	254.5	252.9	251.5	249.3	248.8	248.8	247.8	247.8	247.8	247.5	247.1	247.2	246.2	246.2
0.305	0.250	258.1	257.6	256.1	254.7	252.5	252.0	250.9	250.8	250.8	250.5	250.1	250.1	249.1	249.1	249.1
0.305	0.125	260.8	260.2	258.5	257.4	255.3	254.6	253.5	253.5	253.5	253.1	252.8	252.4	251.4	251.4	251.4
0.356	0.	261.4	260.8	259.4	258.0	255.8	255.0	253.6	253.5	253.2	253.2	252.9	252.4	251.2	251.2	251.2
0.407	0.	259.4	258.9	257.5	256.3	254.0	253.2	251.8	251.5	251.2	251.2	250.8	250.3	249.2	249.2	249.2
0.447	0.500	252.2	251.5	249.9	248.6	246.2	245.7	244.7	244.6	244.6	244.3	243.9	243.9	242.9	242.9	242.9
0.455	0.	258.4	257.7	256.4	254.9	252.8	252.0	250.7	250.3	249.9	249.6	249.2	249.0	247.8	247.8	247.8
0.520	0.	256.1	255.4	254.2	252.7	250.6	249.9	248.5	248.5	247.6	247.2	246.7	246.6	245.4	245.4	245.4
0.520	0.500	251.8	251.1	249.7	248.2	245.9	245.4	244.3	244.0	243.8	243.5	243.1	243.0	241.9	241.9	241.9
0.520	0.375	253.0	252.3	251.0	249.6	247.4	246.8	245.6	245.3	245.0	244.7	244.2	244.1	243.0	243.0	243.0
0.520	0.250	254.2	253.5	252.2	250.9	248.7	248.1	246.8	246.4	246.2	245.8	245.3	245.2	244.1	244.1	244.1
0.520	0.125	255.1	254.4	253.2	251.8	249.6	249.0	247.6	247.2	246.7	246.0	245.9	245.8	244.1	244.1	244.1

Table 3 (cont'd.)  
 TEMPERATURE DISTRIBUTION ON SPHERE-CONE MODEL. (CONE SECTION)  
 MACH NUMBER = 3.03  
 ANGLE OF ATTACK = 6 DEGREES  
 SUPPLY PRESSURE = 980 MILLIMETERS OF HG.  
 SUPPLY TEMPERATURE = 320.0 DEGREES KELVIN

S/R	0	ROLL ANGLE (DEGREES)									135	150	165	180
		0	15	30	45	60	75	90	105	120				
0.645	0°	254.4	253.9	252.5	251.1	249.0	248.2	246.9	246.2	245.7	244.7	244.5	243.3	
0.645	0.500	251.5	250.2	248.1	245.8	245.1	244.1	243.5	243.2	242.8	242.3	242.0	241.2	
0.769	0°	253.7	253.4	251.9	250.5	248.4	247.6	245.6	245.2	244.7	244.1	243.5	243.3	242.1
0.769	0.500	251.0	250.7	249.1	247.8	245.4	244.8	243.6	242.8	242.4	241.9	241.5	240.4	
0.894	0°	253.6	253.1	251.3	249.8	247.7	246.8	245.2	244.2	243.6	242.9	242.3	241.5	
0.894	0.500	251.4	250.8	248.8	247.2	245.0	244.2	242.7	242.0	241.4	240.7	240.3	238.3	239.9
1.018	0°	253.4	253.3	250.9	249.1	247.0	245.9	244.2	243.0	242.5	241.7	241.0	240.9	239.6
1.018	0.500	251.3	251.0	248.4	246.4	244.3	243.3	241.6	240.7	240.3	239.5	239.0	239.1	237.9
1.143	0°	253.3	252.8	250.6	248.6	246.5	245.3	243.5	242.3	241.5	240.8	240.0	239.9	238.6
1.143	0.500	251.3	251.3	247.9	245.1	243.6	242.4	240.7	239.7	239.2	238.6	237.9	238.0	236.8
1.267	0°	253.3	252.3	250.7	250.3	248.1	245.9	244.5	242.7	241.3	240.4	239.7	238.9	237.2
1.267	0.500	251.6	250.9	247.9	245.7	243.5	242.0	240.5	239.2	238.6	238.0	237.4	237.3	236.1
1.392	0°	254.0	253.3	250.6	248.2	245.9	244.3	242.5	241.0	240.0	239.3	238.7	238.3	236.9
1.392	0.500	252.1	251.1	248.0	245.8	243.4	241.8	240.2	238.9	238.0	237.4	237.0	236.7	235.4
1.516	0°	254.7	253.9	250.8	248.2	245.7	243.9	242.1	240.6	239.5	238.7	238.1	237.5	236.0
1.516	0.500	252.9	251.8	248.3	245.7	243.1	241.4	239.7	236.3	237.2	236.6	236.2	235.6	234.3
1.640	0°	255.7	254.8	251.3	250.6	248.4	245.6	243.7	242.0	240.3	239.0	238.1	237.6	235.1
1.640	0.500	252.7	249.9	245.0	243.0	241.0	239.5	238.1	236.1	235.7	235.0	234.8	233.4	
1.765	0°	256.9	255.9	252.2	248.8	245.5	243.6	241.7	240.0	238.6	237.4	236.9	236.0	234.2
1.765	0.500	255.1	253.8	249.7	246.1	242.7	240.6	239.1	237.6	236.4	235.2	235.1	234.0	232.4
1.890	0°	257.8	256.9	253.8	250.9	249.0	245.2	243.0	241.1	239.4	238.0	236.4	235.8	233.0
1.890	0.500	256.5	255.3	250.7	246.6	242.8	240.5	238.8	237.4	236.1	234.9	234.4	233.4	
2.014	0°	259.3	258.3	253.8	250.8	249.6	245.5	243.0	241.0	239.0	237.8	236.3	235.5	232.5
2.014	0.500	258.1	256.9	251.8	247.3	242.9	240.4	238.7	237.2	236.0	234.5	233.7	232.1	231.2
2.138	0°	260.7	259.6	254.9	250.2	245.6	242.9	240.8	239.0	237.7	236.1	233.7	233.0	231.9
2.138	0.500	259.7	258.4	253.3	248.1	243.3	240.6	238.6	237.1	235.9	234.4	234.0	233.0	
2.263	0°	262.2	261.1	256.3	250.8	246.0	243.0	240.7	239.0	237.8	236.1	232.3	231.7	231.4
2.263	0.500	261.2	260.0	254.7	248.7	243.6	240.6	239.5	237.0	235.9	234.6	233.5	233.0	230.3
2.387	0°	263.6	262.6	257.8	251.8	246.5	243.5	241.0	239.4	238.3	236.8	236.0	235.6	231.6
2.387	0.500	262.6	261.4	256.3	249.6	244.0	240.9	238.6	237.1	235.9	234.7	234.3	232.3	230.8
2.512	0°	264.7	263.6	259.0	252.7	246.9	243.6	240.5	239.5	237.6	235.4	234.7	232.9	231.4
2.512	0.500	264.0	262.7	257.8	250.8	244.7	241.3	238.9	237.6	235.8	234.5	233.1	231.8	230.5
2.636	0°	265.8	264.7	260.2	253.9	247.5	244.0	241.4	240.0	239.2	238.6	235.9	233.6	231.8
2.636	0.500	265.1	264.0	259.1	252.1	245.3	241.7	239.2	237.9	236.4	235.7	234.0	232.2	230.8
2.761	0°	266.6	265.6	261.2	255.0	248.4	244.5	242.1	240.8	240.3	237.8	234.5	232.4	231.2
2.761	0.500	265.8	264.7	260.0	253.3	246.0	242.1	239.6	238.4	237.4	235.3	232.9	231.2	
2.885	0°	267.0	266.3	261.7	256.3	249.9	245.7	243.8	242.7	242.5	242.0	241.7	237.5	234.3
3.010	0°	267.5	265.5	264.7	260.8	255.3	248.4	243.9	240.6	240.5	240.7	239.3	235.9	
3.010	0.375	265.5	264.7	260.9	255.4	248.7	244.4	242.3	241.1	241.0	241.4	240.0	235.7	
3.010	0.250	265.7	264.9	260.9	255.4	249.4	245.0	243.0	241.8	241.7	242.2	241.0	237.1	
3.010	0.125	265.9	265.3	261.4	255.9	249.4	245.1	243.0	241.8	241.7	242.2	241.0	237.1	

**Table 4**  
**HEAT TRANSFER COEFFICIENT ON SPHERE-CONE MODEL, (NOSE SECTION)**

MACH NUMBER = 4.0  
 ANGLE OF ATTACK = 18.0 DEGREES  
 SUPPLY PRESSURE = 2C9C.C MILLIMETERS OF HG.  
 SUPPLY TEMPERATURE = 32C.0 DEGREES KELVIN

RCLL ANGLE	DIMENSIONLESS CONE CLR LENGTH (NUSSLETT NO.) / (SQUARE RCT) CF REYNOLDS NO.)					
	C.411	C.356	C.3C1	C.246	0.192	0.137
0.	0.2562	C.327C	0.393 <sup>2</sup>	C.4811	C.5529	0.6032
15.	C.2616	C.319C	C.3855	C.4512	C.514C	0.5710
30.	C.2293	C.29C9	C.3571	C.43EE	C.5CC6	0.5331
45.	C.1888	C.2429	C.3237	C.3987	C.4497	0.5014
60.	C.2C65	C.2115	0.2971	0.3664	0.4709	0.5058
75.	C.1558	C.195 <sup>2</sup>	C.2637	C.341 <sup>2</sup>	C.43C6	0.4979
90.	0.1156	C.1627	C.2163	0.285E	0.3392	0.3894
105.	C.CE25	C.11E2	0.166C	0.24CC	0.3214	0.3795
120.	C.C694	C.1C54	C.1617	0.22C5	0.294C	0.3502
135.	C.C641	C.CE51	C.1371	0.1852	C.253E	0.3287
150.	0.C629	C.C915	0.1256	C.1933	0.2654	0.3216
165.	C.C698	C.07CC	0.C987	C.1581	C.2156	0.2986
180.	C.C651	C.C815	C.11C5	C.157C	C.2286	0.2916

Table 4 (cont'd.)  
 HEAT TRANSFER COEFFICIENT ON SPHERE-CONE MODEL, (CONE SECTION)

MACH NUMBER = 4.8  
 ANGLE OF ATTACK = 15.0 DEGREES  
 SUPPLY PRESSURE = 2090 C.C. MILLIPETERS OF HG.  
 SUPPLY TEMPERATURE = 320 C.C. DEGREES KELVIN

RCLL ANGLE	DIMENSIONLESS CONIC CLR LENGTH						1.640
	C.769	C.894	1.016	1.143	1.267	1.392	
(NUSSELT NO.)/(SQUARE RCCT CF REYNOLDS NO.)							
0.	C.2207	C.1341	C.1378	0.121C	C.1185	0.1286	0.1039
15.	C.1559	C.1544	C.1372	0.125E	C.1325	0.1185	0.1334
30.	C.1699	C.1173	1.5136	C.1078	C.1132	0.1061	0.1275
45.	C.1484	C.993	C.1093	C.1044	C.10CC	0.1138	0.0932
60.	C.1365	C.747	C.895	C.07EE	C.0E22	C.0981	0.0710
75.	C.0824	C.748	C.08C2	C.0776	C.061C	C.0784	0.0477
90.	C.0957	C.542	C.651	C.0442	C.0495	0.0585	0.0568
105.	C.1006	C.0469	C.0435	C.0276	C.0414	0.0417	0.0260
120.	C.0521	C.0324	C.0401	0.0311	C.0346	C.0366	0.0197
135.	C.0746	C.0291	C.0400	0.0324	C.0325	C.0333	0.0183
150.	C.044C	C.0305	C.0423	0.0358	C.0288	0.03C3	0.0158
165.	C.0726	C.0211	C.0446	C.0377	C.0254	C.0257	0.0177
180.	C.0723	0.0223	C.04CE	C.0394	C.0242	C.0267	0.0109
							0.0322
							0.0242
(NUSSELT NO.)/(SQUARE RCCT CF REYNOLDS NO.)							
0.	1.690	2.614	2.138	2.263	2.387	2.512	2.636
15.	C.129C	C.1126	C.1112	C.101E	C.1261	0.0901	0.1044
30.	C.148C	0.1331	0.1368	0.1417	0.1144	0.1545	0.1362
45.	C.1298	0.1240	C.1266	C.1155	0.1131	0.1205	0.1038
60.	C.1176	0.0995	C.1257	C.0968	C.0967	C.0921	0.0903
75.	C.1C17	C.0764	C.0921	C.0842	C.0829	C.0515	0.0804
90.	0.08C1	0.0692	C.0740	C.0667	C.0642	C.0785	0.0608
105.	C.0591	C.0480	C.0524	C.0542	C.0502	0.0666	C.0466
120.	C.0468	C.0231	C.038C	C.0434	C.0316	C.0467	0.0346
135.	C.0451	C.0223	C.0235	0.0339	C.0214	0.0373	0.0212
150.	C.0366	C.0238	C.0243	0.0272	0.0187	0.0327	0.0198
165.	C.0375	C.0253	C.017C	0.0182	0.0091	0.0294	0.0159
180.	C.036C	C.0268	C.0338	C.0195	C.0182	0.0247	0.0200
	C.0351	C.0160	C.0285	C.0222	C.0352	0.0195	0.0158
							0.0356
							0.0025

NOLTR 62-35

FEAT TRANSFER COEFFICIENT ON SPHERE-CONE MCCEL, INCSE SECTION  
Table 4 (cont'd.)

MACH NUMBER = 2.2  
ANGLE OF ATTACK = 12.0 DEGREES  
SUPPLY PRESSURE = 98C.C MILLIMETERS OF HG.  
SUPPLY TEMPERATURE = 31E.C DEGREES KELVIN

RCLL ANGLE	C.465	C.411	C.356	C.301	C.246	C.172	C.137	C.082	C.027
(ASSUMING AC-1 IS SQUARE RCCY CF REYNOLDS 'NC-1')									
0.	C.2125	C.3722	C.4710	C.5296	C.5911	C.64CC	C.6104	0.5765	
15.	C.2162	C.2932	C.4759	C.5445	C.5703	C.6278	C.6054	0.5827	
30.	C.2296	C.3001	C.3835	C.4454	C.5623	C.6079	C.6117	0.6011	
45.	C.1922	C.2562	C.3255	C.4620	C.5164	C.5931	C.6272	0.5827	
60.	C.1661	C.2263	C.2946	C.3621	C.4288	C.4888	C.55C8	0.5796	0.5978
75.	C.1237	C.2038	C.2691	C.3290	C.4102	C.4635	C.5293	0.5715	0.5959
90.	C.1220	C.1690	C.2316	C.2966	C.3604	C.4195	C.5007	0.5729	0.5981
105.	C.CEE9	C.1410	C.1967	C.2512	C.3126	C.3763	C.4549	0.5128	0.5780
120.	C.6576	C.1597	C.1667	C.2265	C.2890	C.3647	C.4433	0.5090	0.5554
135.	0.C460	C.0E59	C.1346	C.2022	C.27C2	C.3319	C.41C0	0.4682	0.5267
150.	C.C460	C.0722	C.1150	C.1855	C.2461	C.3004	C.3939	0.4657	0.5346
165.	C.C3E2	C.0667	C.1562	C.15C2	C.239E	C.3030	C.3751	0.4544	0.5309
180.	C.C364	C.0654	C.1044	C.1576	C.2045	C.2871	C.365C	0.4513	0.5374

HEAT TRANSFER COEFFICIENT ON SPHERE-CCNE MC DLL. (CCNE SECTION.)

MACH NUMBER = 1.2  
 ANGLE OF ATTACK = 10.0 DEGREES  
 SUPPLY PRESSURE = 980.0 MILLIMETERS OF HG.  
 SUPPLY TEMPERATURE = 310.0 DEGREES KELVIN

Table 4 (cont'd.)

RCLL ANGLE	C.645	DIMENSIONLESS CONICAL LENGTH						1.516	1.640
		C.767	C.894	1.016	1.143	1.267	1.392		
(NUSSELT NO.)/(SQUARE RCCI CF REYNOLDS NO.)									
C.	C.1094	C.C478	C.1CE4	C.1151	C.1102	C.1165	C.1140	0.1165	0.1218
15.	C.1098	0.1881	0.1117	0.1375	C.142C	C.1393	0.1453	0.1434	0.1408
30.	C.1078	C.1CE7	C.1176	C.1284	C.1278	C.1217	C.1211	0.1261	0.1212
45.	C.1071	C.1996	C.1CE2Y	C.113C	C.1167	C.1166	C.1111	0.1115	0.1086
60.	C.1078	C.1078	C.1CE9	C.0CE72	C.0CEE3	C.0CE93	C.0CE23	0.0919	0.0856
75.	C.1074	C.1CE47	C.1174	C.1791	C.1792	C.077E	C.0767	0.0752	0.0775
90.	C.1072	C.1CE7C	C.1177	C.1641	C.1595	C.0667	C.0671	0.0712	0.0756
105.	C.1070	C.1CE7C	C.1239	C.144C	C.144C	C.0412	C.0504	0.0412	0.0427
120.	C.1072	C.132	C.1307	C.0201	C.01E5	C.0159	C.0216	0.0218	0.0261
135.	C.1071	C.1171	C.1996	C.013E	C.0253	C.0315	C.0322	C.0348	0.0319
150.	C.1077	C.1CE2Z	C.1241	C.0221	C.1167	C.0249	C.0266	C.0295	0.0397
165.	C.1077	C.1297	C.1281	C.0205	C.0227	C.0229	C.0095	C.0084	0.0454
180.	C.1075	C.1375	C.025E	C.0165	C.0241	C.0402	C.0296	C.0251	0.0491
						•			0.0343
									0.0175
(NUSSELT NO.)/(SQUARE RCCI CF REYNOLDS NO.)									
RCLL ANGLE	1.890	2.014	2.13E	2.262	2.387	2.512	2.636	2.761	2.885
C.	1.122	C.1204	C.1062	C.1136	C.0902	C.0922	C.1056	0.1101	0.0990
15.	C.1273	C.122C	C.1159	C.1265	C.1344	C.1165	C.1186	0.1035	0.0892
30.	C.1198	C.113E	C.1019	C.0917	C.0943	C.0950	C.11C9	0.1010	0.0950
45.	C.105C	C.11C1	C.1086	C.0991	C.0967	C.0939	C.0980	0.1120	0.1048
60.	C.0979	C.0972	C.0975	C.0965	C.0867	C.0912	C.1037	C.0944	0.1097
75.	C.0824	C.09C8	C.0995	C.1215	C.1762	C.1931	C.2155	C.2386	0.2454
90.	C.0855	C.12C6	C.15C2	C.159E	C.1729	C.1737	C.1768	C.1678	0.1623
105.	C.07C7	C.1CE4C	C.0923	C.1C2C	C.1C9C	C.1122	C.1099	C.1122	0.1158
120.	C.05CE	C.0477	C.0547	C.0572	C.0CE72	C.0734	C.0690	C.0741	0.0822
135.	C.04E4	C.0494	C.0616	C.1034	C.2323	C.1CT7	C.0680	C.0615	0.0683
150.	C.0674	C.0742	C.0772	C.078E	C.0770	C.0720	C.0621	C.0707	0.0816
165.	C.04C1	C.0600	C.0823	C.1034	C.1C25	C.1CT7	C.1047	C.1026	0.1065
180.	C.017C	C.02C2	C.029E	C.058E	C.0592	C.0695	C.0763	C.0823	0.0939

**Table 4 (cont'd.)**  
 FLAT TRANSFER COEFFICIENT ON SPHERE-CONE MODEL. (INCSE SECTION)

MACH NUMBER = 5.2  
 ANGLE OF ATTACK = 6.0 DEGREES  
 SUPPLY PRESSURE = 960.0 MILLIMETERS OF HG.  
 SUPPLY TEMPERATURE = 216.0 DEGREES KELVIN

ROLL ANGLE	DIMENSIONLESS CONTOUR LENGTH								
	C.465	C.411	C.356	C.301	C.246	C.192			
(LUSSEAU NO. 1) (SQUARE ROOT REYNOLDS NO.)									
0.	C.1826	C.2250	C.3056	C.4945	C.4761	0.534	0.6032	0.6103	0.6142
15.	C.1574	C.2241	C.2981	C.4642	C.4642	0.5324	C.5879	C.6046	0.6183
30.	C.1659	C.2174	C.2924	0.3814	C.4457	0.5136	0.5618	0.5854	0.6068
45.	C.1284	C.2090	0.2717	C.3416	0.4202	0.4726	0.5307	0.5448	0.5781
60.	C.1671	C.1969	C.2521	C.2994	C.3752	0.4385	C.4674	0.4904	0.5525
75.	C.1439	C.1734	C.2271	0.2934	C.3538	C.4123	C.4672	0.4897	0.5499
90.	C.1356	C.1746	C.2212	C.2224	C.3602	C.4236	C.4768	0.4940	0.5452
105.	C.1171	C.1590	C.2125	C.2886	C.3611	C.4276	C.4832	0.5250	0.5603
120.	C.1162	C.1566	C.2050	C.2852	C.3482	C.4336	C.4920	0.5454	
135.	C.1062	C.1674	C.1966	C.2827	C.3509	C.4443	C.5016	0.5592	0.5812
150.	C.1070	C.1482	C.2024	C.2811	C.3581	C.4310	C.4970	0.5684	0.5875
165.	C.0958	C.1477	C.1986	C.2836	0.3565	C.4276	C.5073	0.5733	0.5912
180.	C.0939	C.1442	C.2046	C.2878	C.3600	C.4312	C.5096	0.5749	0.5924

NOLTR 62-35

Table 4 (cont'd.)  
HEAT TRANSFER COEFFICIENT ON SEMI-ECCENTRIC CYLINDER SECTION

MACH NUMBER = 3.2  
ANGLE OF ATTACK = 6.0 DEGREES  
SUPPLY PRESSURE = 980.0 MILLIMETERS OF HG.  
SUPPLY TEMPERATURE = 31E. C DEGREES KELVIN

RCLL ANGLE	DIMENSIONS ON PLATE OF REYACLES NO. 1									
	C. 0.762	C. 0.874	C. 0.918	C. 1.142	C. 1.267	C. 1.392	C. 1.516	C. 1.640	C. 1.764	C. 1.888
C.	C. C9E2	C. C817	C. C7C2	C. C745	C. C575	C. C713	C. C694	C. C744	C. C694	C. C744
15.	C. C9S2	C. C913	C. C736	C. C15C	C. C8C6	C. C707	C. C816	C. C318	C. JE60	C. JE60
3C.	C. C847	C. C836	C. C741	C. C7C6	C. C791	C. C62C	C. C656	C. C656	C. U680	C. U680
45.	C. C5CE	C. C1C55	C. C942	C. C875	C. C596	C. C717	C. C8C3	C. C758	C. U788	C. U788
EC.	C. C65C	C. C712	C. C66C	C. C677	C. C78C	C. C755	C. C7C0	C. C675	C. U730	C. U730
75.	C. C72C	C. C807	C. C735	C. C712	C. C782	C. U585	C. C669	C. C628	C. U689	C. U689
9C.	C. C752	C. C771	C. C694	C. C736	C. C591	C. C622	C. C622	C. U722	C. U722	C. U722
1C5.	C. C1E7	C. C652	C. C4C2	C. C564	C. C74E	C. U455	C. C5E1	C. C578	C. U591	C. U591
12C.	C. C671	C. C618	C. C612	C. C6C2	C. C612	C. C528	C. C541	C. U518	C. U518	C. U518
135.	C. C664	C. C5C8	C. C629	C. C481	C. C522	C. C356	C. U459	C. U470	C. U468	C. U468
150.	C. C922	C. C527	C. C535	C. C519	C. C492	C. C3C7	C. C5C1	C. U500	C. U552	C. U552
165.	C. C394	C. C453	C. C444	C. C448	C. C432	C. C45E	C. C267	C. U425	C. U409	C. U409
18C.	C. C444	C. C197	C. C451	C. C325	C. U394	C. C42	C. C172	C. C135	C. U363	C. U363

ROLL ANGLE	ROLL ANGLE	CIPENSICLER LENGTH			CIPENSICLER LENGTH					
		1.765	1.890	2.014	2.128	2.263	2.397	2.512	2.635	2.761
(ALSELT AC.)/(SQUARE RCCT CF REYACLES NC.)										
C.	C.0584	C.0524	C.0549	C.0602	C.0575	C.0497	C.0581	C.0497	C.0577	C.0657
15.	C.0738	C.0669	C.0660	C.0759	C.0570	C.0594	C.0657	C.0648	C.0648	C.0587
30.	C.0602	C.0545	C.0577	C.0657	C.0566	C.0605	C.0605	C.0639	C.0539	C.0587
45.	C.0688	C.0655	C.0625	C.0680	C.0605	C.0625	C.0675	C.0675	C.0569	C.0569
60.	C.0722	C.0655	C.0622	C.0648	C.0570	C.0529	C.0598	C.0598	C.0733	C.0733
75.	C.0644	C.0542	C.0552	C.0692	C.0563	C.0576	C.0598	C.0598	C.0600	C.0600
90.	C.0613	C.0675	C.0595	C.0672	C.0523	C.0550	C.0674	C.0674	C.0664	C.0664
105.	C.0670	C.0542	C.0494	C.0608	C.0476	C.0499	C.0588	C.0588	C.0689	C.0689
120.	C.0572	C.0494	C.0479	C.0586	C.0456	C.0496	C.0551	C.0551	C.0752	C.0752
135.	C.0490	C.0493	C.0370	C.0392	C.0540	C.0479	C.0611	C.0611	C.0745	C.0917
150.	C.0561	C.0382	C.0344	C.0293	C.0297	C.0292	C.0433	C.0433	C.0665	C.0957
165.	C.0489	C.0324	C.0159	C.0201	C.0191	C.0327	C.0144	C.0144	C.0276	C.0366
180.	C.0368	C.0164	C.0262	C.0196	C.0218	C.0144	C.0245	C.0245	C.0355	C.1096

NOLTR 62-35

AERODYNAMICS DEPARTMENT  
EXTERNAL DISTRIBUTION LIST (A1)

	<u>No. of Copies</u>
Chief, Bureau of Naval Weapons Department of the Navy Washington 25, D. C. Attn: DLI-30 Attn: R-14 Attn: RRRE-4 Attn: RMGA-413	1 1 1 1
Office of Naval Research Room 2709, T-3 Washington 25, D. C. Attn: Head, Mechanics Branch	1
Director, David Taylor Model Basin Aerodynamics Laboratory Washington 7, D. C. Attn: Library	1
Commander, U. S. Naval Ordnance Test Station China Lake, California Attn: Technical Library Attn: Code 503 Attn: Code 406	1 1 1
Director, Naval Research Laboratory Washington 25, D. C. Attn: Code 2027	1
Commanding Officer Office of Naval Research Branch Office Box 39, Navy 100 Fleet Post Office New York, New York	1
NASA High Speed Flight Station Box 273 Edwards Air Force Base, California Attn: W. C. Williams	1
NASA Ames Research Center Moffett Field, California Attn: Librarian	1

**AERODYNAMICS DEPARTMENT  
EXTERNAL DISTRIBUTION LIST (A1)**

	<u>No. of Copies</u>
<b>NASA</b> Langley Research Center Langley Field, Virginia	
Attn: Librarian	3
Attn: C. H. McLellan	1
Attn: J. J. Stack	1
Attn: Adolf Busemann	1
Attn: Comp. Res. Div.	1
Attn: Theoretical Aerodynamics Division	1
<b>NASA</b> Lewis Research Center 21000 Brookpark Road Cleveland 11, Ohio	
Attn: Librarian	1
Attn: Chief, Propulsion Aerodynamics Div.	1
<b>NASA</b> 1520 H Street, N. W. Washington 25, D. C.	
Attn: Chief, Division of Research Information	1
Attn: Dr. H. H. Kurzweg, Asst. Director of Research	1
<b>Office of the Assistant Secretary of Defense (R&amp;D)</b> Room 3E1065, The Pentagon Washington 25, D. C.	
Attn: Technical Library	1
<b>Research and Development Board</b> Room 3D1041, The Pentagon Washington 25, D. C.	
Attn: Library	1
<b>ASTIA</b> Arlington Hall Station Arlington 12, Virginia	10
<b>Commander, Pacific Missile Range</b> Point Mugu, California	
Attn: Technical Library	1
<b>Commanding General</b> Aberdeen Proving Ground, Maryland	
Attn: Technical Information Branch	1
Attn: Ballistic Research Laboratory	1

**AERODYNAMICS DEPARTMENT  
EXTERNAL DISTRIBUTION LIST (A1)**

	<u>No. of Copies</u>
Commander, Naval Weapons Laboratory Dahlgren, Virginia Attn: Library	1
Director, Special Projects Department of the Navy Washington 25, D. C. Attn: SP-2722	1
Director of Intelligence Headquarters, USAF Washington 25, D. C. Attn: AFOIN-3B	1
Headquarters - Aero. Systems Division Wright-Patterson Air Force Base Dayton, Ohio Attn: WWAD Attn: RRLA-Library	2 1
Commander Air Force Ballistic Missile Division HQ Air Research & Development Command P. O. Box 262 Inglewood, California Attn: WDTLAR	1
Chief, Defense Atomic Support Agency Washington 25, D. C. Attn: Document Library	1
Headquarters, Arnold Engineering Development Center Air Research and Development Center Arnold Air Force Station, Tennessee Attn: Technical Library Attn: AEOR Attn: AEOIM	1 1 1
Commanding Officer, DOFL Washington 25, D. C. Attn: Library, Room 211, Bldg. 92	1
Commanding General Redstone Arsenal Huntsville, Alabama Attn: Mr. N. Shapiro (ORDDW-MRF) Attn: Technical Library	1 1

NOLTR 62-35

AERODYNAMICS DEPARTMENT  
EXTERNAL DISTRIBUTION LIST (A1)

	<u>No. of Copies</u>
<b>NASA</b> George C. Marshall Space Flight Center Huntsville, Alabama	
Attn: Dr. E. Geissler	1
Attn: Mr. T. Reed	1
Attn: Mr. H. Paul	1
Attn: Mr. W. Dahm	1
Attn: Mr. D. Burrows	1
Attn: Mr. J. Kingsbury	1
Attn: ORDAB-DA	1
 <b>APL/JHU (C/NOW 7386)</b> 8621 Georgia Avenue Silver Spring, Maryland	
Attn: Technical Reports Group	2
Attn: Mr. Fox	1
Attn: Dr. F. Hill	1
Via: INSORD	
 <b>Air Force Systems Command</b> Scientific & Technical Liaison Office Room 2305, Munitions Building Department of the Navy Washington 25, D. C.	
Attn: E. G. Haas	1

NOLTR 62-35

AERODYNAMICS DEPARTMENT  
EXTERNAL DISTRIBUTION LIST (A2)

	<u>No. of Copies</u>
University of Minnesota Minneapolis 14, Minnesota Attn: Dr. E. R. G. Eckert Attn: Heat Transfer Laboratory Attn: Technical Library	1 1 1
Rensselaer Polytechnic Institute Troy, New York Attn: Dept. of Aeronautical Engineering	1
Dr. James P. Hartnett Department of Mechanical Engineering University of Delaware Newark, Delaware	1
Princeton University James Forrestal Research Center Gas Dynamics Laboratory Princeton, New Jersey Attn: Prof. S. Bogdonoff Attn: Dept. of Aeronautical Engineering Library	1 1
Defense Research Laboratory The University of Texas P. O. Box 8029 Austin 12, Texas Attn: Assistant Director	1
Ohio State University Columbus 10, Ohio Attn: Security Officer Attn: Aerodynamics Laboratory Attn: Dr. J. Lee Attn: Chairman, Dept. of Aero. Engineering	1 1 1 1
California Institute of Technology Pasadena, California Attn: Guggenheim Aero. Laboratory, Aeronautics Library Attn: Jet Propulsion Laboratory Attn: Dr. H. Liepmann Attn: Dr. L. Lees Attn: Dr. D. Coles Attn: Mr. A. Roshko Attn: Dr. J. Laufer	1 1 1 1 1 1 1 1
Case Institute of Technology Cleveland 6, Ohio Attn: G. Kuerti	1

**AERODYNAMICS DEPARTMENT  
EXTERNAL DISTRIBUTION LIST (A2)**

	<u>No. of Copies</u>
North American Aviation, Inc. Aerophysics Laboratory Downing, California Attn: Dr. E. R. Van Driest Attn: Missile Division (Library)	1 1
Department of Mechanical Engineering Yale University 400 Temple Street New Haven 10, Connecticut Attn: Dr. P. P. Wegener Attn: Prof. N. A. Hall	1 1
MIT Lincoln Laboratory Lexington, Massachusetts	1
RAND Corporation 1700 Main Street Santa Monica, California Attn: Library, USAF Project RAND Attn: Technical Communications	1 1
Mr. J. Lukasiewicz Chief, Gas Dynamics Facility ARO, Incorporated Tullahoma, Tennessee	1
Massachusetts Institute of Technology Cambridge 39, Massachusetts Attn: Prof. J. Kaye Attn: Prof. M. Finston Attn: Mr. J. Baron Attn: Prof. A. H. Shapiro Attn: Naval Supersonic Laboratory Attn: Aero. Engineering Library	1 1 1 1 1 1
Polytechnic Institute of Brooklyn 527 Atlantic Avenue Freeport, New York Attn: Dr. A. Ferri Attn: Dr. M. Bloom Attn: Dr. P. Libby Attn: Aerodynamics Laboratory	1 1 1 1
Brown University Division of Engineering Providence, Rhode Island Attn: Prof. R. Probstein Attn: Prof. C. Lin Attn: Librarian	1 1 1

NOLTR 62-35

AERODYNAMICS DEPARTMENT  
EXTERNAL DISTRIBUTION LIST (A2)

	No. of Copies
Air Ballistics Laboratory Army Ballistic Missile Agency Huntsville, Alabama	1
Applied Mechanics Reviews Southwest Research Institute 8500 Culebra Road San Antonio 6, Texas	1
BuWeps Representative Aerojet-General Corporation 6352 N. Irwindale Avenue Azusa, California	1
Boeing Airplane Company Seattle, Washington Attn: J. H. Russell Attn: Research Library	1 1
United Aircraft Corporation 400 Main Street East Hartford 8, Connecticut Attn: Chief Librarian Attn: Mr. W. Kuhrt, Research Dept. Attn: Mr. J. G. Lee	1 2 1
Hughes Aircraft Company Florence Avenue at Teale Streets Culver City, California Attn: Mr. D. J. Johnson R&D Technical Library	1
McDonnell Aircraft Corporation P. O. Box 516 St. Louis 3, Missouri	1
Lockheed Missiles and Space Company P. O. Box 504 Sunnyvale, California Attn: Dr. L. H. Wilson Attn: Mr. M. Tucker Attn: Mr. R. Smelt	1 1 1
The Martin Company Baltimore 3, Maryland Attn: Library Attn: Chief Aerodynamicist	1 1

**AERODYNAMICS DEPARTMENT  
EXTERNAL DISTRIBUTION LIST (A2)**

	<u>No. of Copies</u>
<b>CONVAIR</b> A Division of General Dynamics Corporation Fort Worth, Texas Attn: Library 1 Attn: Theoretical Aerodynamics Group 1	
<b>Purdue University</b> School of Aeronautical & Engineering Sciences LaFayette, Indiana Attn: R. L. Taggart, Library 1	
<b>University of Maryland</b> College Park, Maryland Attn: Director 2 Attn: Dr. J. Burgers 1 Attn: Librarian, Engr. & Physical Sciences 1 Attn: Librarian, Institute for Fluid Dynamics and Applied Mathematics 1	
<b>University of Michigan</b> Ann Arbor, Michigan Attn: Dr. A. Kuethe 1 Attn: Dr. O. Laporte 1 Attn: Department of Aeronautical Engineering 1	
<b>Stanford University</b> Palo Alto, California Attn: Applied Mathematics & Statistics Lab. 1 Attn: Prof. D. Bershad, Dept. of Aero. Engr. 1	
<b>Cornell University</b> Graduate School of Aeronautical Engineering Ithaca, New York Attn: Prof. W. R. Sears 1	
<b>The Johns Hopkins University</b> Charles and 34th Streets Baltimore, Maryland Attn: Dr. F. H. Clauser 1 Attn: Dr. M. Morkovin 1	
<b>University of California</b> Berkeley 4, California Attn: G. Maslach 1 Attn: Dr. S. Schaaf 1 Attn: Dr. Holt 1 Attn: Institute of Engineering Research 1	

**AERODYNAMICS DEPARTMENT  
EXTERNAL DISTRIBUTION LIST (A2)**

	<u>No. of Copies</u>
Cornell Aeronautical Laboratory, Inc. 4455 Genesee Street Buffalo 21, New York Attn: Librarian Attn: Dr. Franklin Moore Attn: Dr. J. G. Hall	1 1 1
University of Minnesota Rosemount Research Laboratories Rosemount, Minnesota Attn: Technical Library	1
Director, Air University Library Maxwell Air Force Base, Alabama	1
Douglas Aircraft Company, Inc. Santa Monica Division 3000 Ocean Park Boulevard Santa Monica California Attn: Chief Missiles Engineer Attn: Aerodynamics Section	1 1
General Motors Corporation Defense Systems Division Santa Barbara, California Attn: Dr. A. C. Charters	1
CONVAIR A Division of General Dynamics Corporation Daingerfield, Texas	1
CONVAIR Scientific Research Laboratory 5001 Kearney Villa Road San Diego 11, California Attn: Mr. M. Sibulkin Attn: Asst. to the Director of Scientific Research Attn: Dr. B. M. Leadon Attn: Library	1 1 1 1
Republic Aviation Corporation Farmingdale, New York Attn: Technical Library	1
General Applied Science Laboratories, Inc. Merrick and Stewart Avenues Westbury, L. I., New York Attn: Mr. Walter Daskin Attn: Mr. R. W. Byrne	1 1

**AERODYNAMICS DEPARTMENT  
EXTERNAL DISTRIBUTION LIST (A2)**

	<u>No. of Copies</u>
<b>Arnold Research Organization, Inc.</b> <b>Tullahoma, Tennessee</b>	
Attn: Technical Library	1
Attn: Chief, Propulsion Wind Tunnel	1
Attn: Dr. J. L. Potter	1
<b>General Electric Company</b> <b>Missile and Space Vehicle Department</b> <b>3198 Chestnut Street</b> <b>Philadelphia, Pennsylvania</b>	
Attn: Larry Chason, Mgr. Library	2
Attn: Mr. R. Kirby	1
Attn: Dr. J. Farber	1
Attn: Dr. G. Sutton	1
Attn: Dr. J. D. Stewart	1
Attn: Dr. S. M. Scala	1
Attn: Dr. H. Lew	1
<b>Eastman Kodak Company</b> <b>Navy Ordnance Division</b> <b>50 West Main Street</b> <b>Rochester 14, New York</b>	
Attn: W. B. Forman	2
<b>Library</b> <b>AVCO-Everett Research Laboratory</b> <b>2385 Revere Beach Parkway</b> <b>Everett 49, Massachusetts</b>	3
<b>AVCO-Everett Research Laboratory</b> <b>201 Lowell Street</b> <b>Wilmington, Massachusetts</b>	
Attn: Mr. F. R. Riddell	1
<b>AER, Incorporated</b> <b>158 North Hill Avenue</b> <b>Pasadena, California</b>	1
<b>Armour Research Foundation</b> <b>10 West 35th Street</b> <b>Chicago 16, Illinois</b>	
Attn: Dept. M	2
Attn: Dr. Paul T. Torda	1
<b>Chance-Vought Aircraft, Inc.</b> <b>Dallas, Texas</b>	
Attn: Librarian	2

**AERODYNAMICS DEPARTMENT  
EXTERNAL DISTRIBUTION LIST (A2)**

	<u>No. of Copies</u>
National Science Foundation 1951 Constitution Avenue, N. W. Washington 25, D. C. Attn: Engineering Sciences Division	1
New York University University Heights New York 53, New York Attn: Department of Aeronautical Engineering	1
New York University 25 Waverly Place New York 3, New York Attn: Library, Institute of Math. Sciences	1
NORAIR A Division of Northrop Corp. Hawthorne, California Attn: Library	1
Northrop Aircraft, Inc. Hawthorne, California Attn: Library	1
Gas Dynamics Laboratory Technological Institute Northwestern University Evanston, Illinois Attn: Library	1
Pennsylvania State University University Park, Pennsylvania Attn: Library, Dept. of Aero. Engineering	1
The Ramo-Wooldridge Corporation 8820 Bellanca Avenue Los Angeles 45, California	1
Gifts and Exchanges Fondren Library Rice Institute P. O. Box 1892 Houston 1, Texas	1
University of Southern California Engineering Center Los Angeles 7, California Attn: Librarian	1

AERODYNAMICS DEPARTMENT  
EXTERNAL DISTRIBUTION LIST (A2)

	<u>No. of Copies</u>
Commander Air Force Flight Test Center Edwards Air Force Base Muroc, California Attn: FTOTL	1
Air Force Office of Scientific Research Holloman Air Force Base Alamogordo, New Mexico Attn: SRLTL	1
The Editor Battelle Technical Review Battelle Memorial Institute 505 King Avenue Columbus 1, Ohio	1
Douglas Aircraft Company, Inc. El Segundo Division El Segundo, California	1
Fluidyne Engineering Corp. 5740 Wayzata Blvd. Golden Valley Minneapolis 16, Minnesota	1
Grumman Aircraft Engineering Corp. Bethpage, L. I., New York	1
Lockheed Missile and Space Company P. O. Box 551 Burbank, California Attn: Library	1
Marquardt Aircraft Corporation 7801 Havenhurst Van Nuys, California	1
The Martin Company Denver, Colorado Attn: Library	1
Mississippi State College Engineering and Industrial Research Station Aerophysics Department P. O. Box 248 State College, Mississippi	1

**AERODYNAMICS DEPARTMENT  
EXTERNAL DISTRIBUTION LIST (A2)**

	<u>No. of Copies</u>
Lockheed Missile and Space Company 3251 Hanover Street Palo Alto, California Attn: Mr. J. A. Laurmann Attn: Library	1
General Electric Company Research Laboratory Schenectady, New York Attn: Dr. H. T. Nagamatsu Attn: Library	1
Fluid Dynamics Laboratory Mechanical Engineering Department Stevens Institute of Technology Hoboken, New Jersey Attn: Dr. R. H. Page, Director	1
Department of Mechanical Engineering University of Arizona Tucson, Arizona Attn: Dr. E. K. Parks	1
Vitro Laboratories 200 Pleasant Valley Way West Orange, New Jersey Attn: Dr. Charles Sheer	1
Department of Aeronautical Engineering University of Washington Seattle 5, Washington Attn: Prof. R. E. Street Attn: Library	1 1
Aeronautical Engineering Review 2 East 64th Street New York 21, New York	1
Institute of the Aerospace Sciences 2 East 64th Street New York 21, New York Attn: Managing Editor Attn: Library	1 1
Department of Aeronautics United States Air Force Academy Colorado	1

**AERODYNAMICS DEPARTMENT  
EXTERNAL DISTRIBUTION LIST (A2)**

	<u>No. of Copies</u>
MHD Research, Inc. Newport Beach, California Attn: Dr. V. H. Blackman, Technical Director	1
University of Alabama College of Engineering University, Alabama Attn: Prof. C. H. Bryan, Head Dept. of Aeronautical Engineering	1
Office of Naval Research Bldg. T-3, Department of the Navy 17th and Constitution Avenue Washington 25, D. C. Attn: Mr. Ralph D. Cooper, Head Fluid Dynamics Branch	1
ARDE Associates 100 W. Century Road Paramus, New Jersey Attn: Mr. Edward Cooperman	1
Aeronautical Research Associates of Princeton 50 Washington Road Princeton, New Jersey Attn: Dr. C. duP. Donaldson, President	1
Daniel Guggenheim School of Aeronautics Georgia Institute of Technology Atlanta, Georgia Attn: Prof. A. L. Ducoffe	1
University of Cincinnati Cincinnati, Ohio Attn: Prof. R. P. Harrington, Head Dept. of Aeronautical Engineering	1
Virginia Polytechnic Institute Dept. of Aerospace Engineering Blacksburg, Virginia Attn: Mr. R. T. Keefe Attn: Library	1
IBM Federal System Division 7220 Wisconsin Avenue Bethesda, Maryland Attn: Dr. I. Korobkin	1

NOLTR 62-35

AERODYNAMICS DEPARTMENT  
EXTERNAL DISTRIBUTION LIST (A2)

	<u>No. of Copies</u>
Superintendent U. S. Naval Postgraduate School Monterey, California Attn: Technical Reports Section Library	1
National Bureau of Standards Washington 25, D. C. Attn: Chief, Fluid Mechanics Section	1
North Carolina State College Raleigh, North Carolina Attn: Prof. R. W. Truitt, Head Dept. of Mechanical Engineering	1
Attn: Division of Engineering Research Technical Library	1

## CATALOGING INFORMATION FOR LIBRARY USE

BIBLIOGRAPHIC INFORMATION

Descriptors	Codes	Descriptors	Codes
Source <u>NOL technical report</u>	<u>NONTR</u>	Security Classification and Code Count <u>Inclassified - 23</u>	<u>U023</u>
Report Number <u>62-35</u>	<u>624635</u>	Circulation Limitation	
Report Date <u>8 June 1962</u>	<u>0662</u>	Circulation Limitation or Bibliographic	

SUBJECT ANALYSIS OF REPORT

Descriptors	Codes	Descriptors	Codes	Descriptors	Codes
<u>Bodies</u>	<u>BODY</u>	<u>Laminar</u>	<u>LAMI</u>		
<u>Heat transfer</u>	<u>HEAT</u>	<u>Turbulent</u>	<u>TUBU</u>		
<u>Pressure</u>	<u>PRES</u>	<u>Theory</u>	<u>THEY</u>		
<u>Flow</u>	<u>FLOW</u>	<u>Measurements</u>	<u>MEAU</u>		
<u>Supersonic</u>	<u>SUPR</u>	<u>Testing equipment</u>	<u>TESR</u>		
<u>Aerodynamic</u>	<u>AERD</u>	<u>Wind tunnel</u>	<u>WINU</u>		
<u>Spheres</u>	<u>SPHE</u>	<u>Tests</u>	<u>TEST</u>		
<u>Cones</u>	<u>CONE</u>	<u>Instruments</u>	<u>INSM</u>		
<u>Mach</u>	<u>MACH</u>	<u>Temperature</u>	<u>TEMP</u>		
<u>Number</u>	<u>NUMB</u>	<u>Data reduction</u>	<u>DATR</u>		
<u>3.23</u>	<u>3X00</u>	<u>Bodies (Tests)</u>	<u>BODYT</u>		
<u>4.83</u>	<u>4X75</u>				

Naval Ordnance Laboratory, White Oak, Md.  
(NOL technical report 62-35)  
SUPERSONIC AERODYNAMIC HEAT TRANSFER AND  
PRESSURE DISTRIBUTIONS ON A SPHERE-CONE  
MODEL AT HIGH ANGLES OF YAW, by Lionel  
Pasink. 8 June 1962. 10p. charts, ta-  
bles, diagrs. (Aerodynamics research  
report 174) Task RMGK-42-034/212-1/FO09-  
10-001. UNCLASSIFIED

Measurements of the static pressure and  
aerodynamic heat transfer on the surface  
of a sphere-cone model at Mach numbers of  
3.23 and 4.83, and angles of yaw of 6° and  
18° have been made. The results of sever-  
al theoretical methods for calculating  
both the laminar and turbulent heat trans-  
fer to the body along the most windward  
and leeward streamlines are compared with  
the experimental measurements.

1. Bodies - Heat trans-  
fer  
2. Bodies - Pressure  
3. Bodies - Wind tunnel  
tests  
4. Heat - Transference

Title I. Pasink, Lio-  
nel  
III. Series Project

Naval Ordnance Laboratory, White Oak, Md.  
(NOL technical report 62-35)  
SUPERSONIC AERODYNAMIC HEAT TRANSFER AND  
PRESSURE DISTRIBUTIONS ON A SPHERE-CONE  
MODEL AT HIGH ANGLES OF YAW, by Lionel  
Pasink. 8 June 1962. 10p. charts, ta-  
bles, diagrs. (Aerodynamics research  
report 174) Task RMGK-42-034/212-1/FO09-  
10-001. UNCLASSIFIED

Measurements of the static pressure and  
aerodynamic heat transfer on the surface  
of a sphere-cone model at Mach numbers of  
3.23 and 4.83, and angles of yaw of 6° and  
18° have been made. The results of sever-  
al theoretical methods for calculating  
both the laminar and turbulent heat trans-  
fer to the body along the most windward  
and leeward streamlines are compared with  
the experimental measurements.

1. Bodies - Heat trans-  
fer  
2. Bodies - Pressure  
3. Bodies - Wind tunnel  
tests  
4. Heat - Transference

Title I. Pasink, Lio-  
nel  
III. Series Project

Naval Ordnance Laboratory, White Oak, Md.  
(NOL technical report 62-35)  
SUPERSONIC AERODYNAMIC HEAT TRANSFER AND  
PRESSURE DISTRIBUTIONS ON A SPHERE-CONE  
MODEL AT HIGH ANGLES OF YAW, by Lionel  
Pasink. 8 June 1962. 10p. charts, ta-  
bles, diagrs. (Aerodynamics research  
report 174) Task RMGK-42-034/212-1/FO09-  
10-001. UNCLASSIFIED

1. Bodies - Heat trans-  
fer  
2. Bodies - Pressure  
3. Bodies - Wind tunnel  
tests  
4. Heat - Transference

Title I. Pasink, Lio-  
nel  
III. Series Project

Naval Ordnance Laboratory, White Oak, Md.  
(NOL technical report 62-35)  
SUPERSONIC AERODYNAMIC HEAT TRANSFER AND  
PRESSURE DISTRIBUTIONS ON A SPHERE-CONE  
MODEL AT HIGH ANGLES OF YAW, by Lionel  
Pasink. 8 June 1962. 10p. charts, ta-  
bles, diagrs. (Aerodynamics research  
report 174) Task RMGK-42-034/212-1/FO09-  
10-001. UNCLASSIFIED

Measurements of the static pressure and  
aerodynamic heat transfer on the surface  
of a sphere-cone model at Mach numbers of  
3.23 and 4.83, and angles of yaw of 6° and  
18° have been made. The results of sever-  
al theoretical methods for calculating  
both the laminar and turbulent heat trans-  
fer to the body along the most windward  
and leeward streamlines are compared with  
the experimental measurements.

1. Bodies - Heat trans-  
fer  
2. Bodies - Pressure  
3. Bodies - Wind tunnel  
tests  
4. Heat - Transference

Title I. Pasink, Lio-  
nel  
III. Series Project

Naval Ordnance Laboratory, White Oak, Md.  
(NOL technical report 62-35)  
SUPERSONIC AERODYNAMIC HEAT TRANSFER AND  
PRESSURE DISTRIBUTIONS ON A SPHERE-CONE  
MODEL AT HIGH ANGLES OF YAW, by Lionel  
Pasink. 8 June 1962. 10p. charts, ta-  
bles, diagrs. (Aerodynamics research  
report 174) Task RMGK-42-034/212-1/FO09-  
10-001. UNCLASSIFIED